Structural–metamorphic evolution of the Southern Yenisey Range of Eastern Siberia: Implications for the emplacement of the Kanskiy granulite Complex

Article *in* Mineralogy and Petrology · May 2000

DOI: 10.1007/s007100050018

CITATIONS
31

READS
69

5 authors, including:

Dirk Daniel van Reenen
University of Johannesburg
123 PUBLICATIONS **3,012** CITATIONS

SEE PROFILE

D. A. Varlamov
Russian Academy of Sciences
132 PUBLICATIONS **460** CITATIONS

SEE PROFILE

Mineralogy and Petrology (2000) 69: 35–67

Mineralogy and Petrology

Structural-metamorphic evolution of the Southern Yenisey Range of Eastern Siberia: implications for the emplacement of the Kanskiy granulite Complex

C. A. Smit[1], **D. D. Van Reenen**[1], **T. V. Gerya**[2], **D. A. Varlamov**[2], and **A. V. Fed'kin**[2]

[1] Department of Geology, Rand Afrikaans University, Auckland Park, South Africa
[2] Institute of Experimental Mineralogy, Russian Academy of Sciences, Chernogolovka, Moscow district, Russia

With 10 Figures

Received April 27, 1999;
revised version accepted July 14, 1999

Summary

The Southern Yenisey Range of Eastern Siberia consists of the granulite facies Kanskiy Complex bordered in the west by the lower-grade Yeniseyskiy and Yukseevskiy Complexes. Three deformational events were recognized in each of the three complexes along the Yenisey River cross-section: a D1 fabric forming event, a D2 shear and folding event, and a D3 shear event. Thrust kinematics across the Southern Yenisey Range suggest that during the D2 event the Kanskiy Complex was thrusted along a regional ductile shear zone onto the lower-grade complexes. This resulted in shearing and folding as well as the development of a dynamic metamorphic zonation. In the low-grade greenstone belt part of the cross section (Yukseevskiy complex) D2 shearing is associated with peak prograde ($T \sim 660\,^{\circ}C$ and $P \sim 5.8$ kbar) metamorphism. The retrograde *P-T* path of the Yukseevskiy Complex coincides with minimum *T* of the near-isobaric cooling *P-T* paths for the adjacent granulites of the Kanskiy Complex (*Perchuk* et al., 1989). The metamorphism can therefore be attributed to deformation and heat transfer caused by exhumation of the Kanskiy Complex in the time period 2000–1800 Ma which also defines the most significant tectono-thermal event in the Southern Yenisey Range. The tectono-metamorphic pattern and evolution of the low- to high-grade metamorphic complexes of the Southern Yenisey Range is very similar to that described for the ~2600 Ma Limpopo Complex of Southern Africa and the ~1900 Ma Lapland Complex of the Kola Peninsula. Similar geodynamic processes were therefore possibly responsible for the formation of these high-grade terrains suggesting that their formation is linked to a general geodynamic model.

Zusammenfassung

Strukturelle und metamorphe Entwicklung des südlichen Jenissei-Gebirges in Ost-Sibirien: Bedeutung für die Platznahme des Kanskiy Granulit-Komplexes

Das südliche Jenissei-Gebirge in Ost-Sibirien besteht aus dem granulit-faziellen Kanskiy Komplex, der im Westen durch die niedrig-gradigen Jenisseiski und Jukseevski-Komplexe begrenzt wird. Drei Deformations-Phasen können in jedem der drei Komplexe längs eines Profiles am Jenissei-Fluss beobachtet werden: Eine Phase, die zur Entwicklung des D1 Gefüges führte, eine Phase D2 mit Scher- und Faltvorgängen und eine D3 Scher-Phase. Die Kinematik von Überschiebungen über das südliche Jenissei-Gebirge deuten an, dass während der D2-Phase der Kanskiy-Komplex längs einer regionalen duktilen Scherzone auf die niedriggradigeren Komplexe überschoben wurde. Dies führte zu Scherung und Faltung, sowie zur Entwicklung einer dynamischen metamorphen Zonierung. In dem niedriggradigen Grünsteingürtel innerhalb des Profils (Jukseevski-Komplex) ist D2-Scherung mit dem Höhepunkt der prograden Metamorphose ($T \approx 660\,^{\circ}C$ und $P \approx 5{,}8$ kbar) zusammengefallen. Der retrograde P-T-Pfad des Jukseevski-Komplexes fällt mit der Minimum-Temperatur der fast isobaren Abkühlung der P-T-Pfade für die benachbarten Granulite des Kanskiy-Komplexes zusammen (*Perchuk* et al., 1989). Die Metamorphose kann deshalb auf Deformation und Wärmefluss zurückgeführt werden, die durch die Freilegung des Kanskiy-Komplexes zwischen 2.00 und 1.80 Ma verursacht wurde; letztere fällt auch mit der wichtigsten tektono-thermalen Phase im südlichen Jenissei-Gebirge zusammen. Das tektono-metamorphe Muster und die Entwicklung von niedrig- zu hochgradigen metamorphen Komplexen des südlichen Jenissei-Gebirges ähnelt in vielfältiger Weise dem ungefähr 2.600 Ma alten Limpopo-Komplex im südlichen Afrika und dem 1.900 Ma alten Lappland-Komplex der Kola-Halbinsel. Ähnliche geodynamische Prozesse waren deshalb möglicherweise für die Entstehung dieser hochgradig metamorphen Terrains verantwortlich; dies wiederum weist darauf hin, dass ihre Entstehung einem allgemeinen geodynamischen Modell entspricht.

Abbreviations

Ab albite, *Alm* almandine, *An* anorthite, *And* andalusite, *Bt* biotite, *Chl* chlorite, *Cpx* clinopyroxene, *Crd* cordierite, *Ep* epidote, *Grt* garnet, *Grs* grossular, *Hbl* hornblende, *Kfs* potassium feldspar, *Ky* kyanite, *Mag* magnetite, *Ms* muscovite, *Opx* othopyroxene, *Pl* plagioclase, *Prp* pyrope, *Qtz* quartz, *Sil* sillimanite, *Spl* spinel, *Sps* spessartine, X_i mole fraction of component i in a phase, for example $X_{Mg} = Mg/(Mg + Fe)$; N_i mole per cent of component i in a phase, T temperature, P pressure in kbar.

Introduction

Recent studies of Precambrian granulitic complexes and adjacent lower grade cratonic terrains in Southern Africa and Russia (e.g. *Perchuk*, 1989; *Van Reenen* et al., 1990; *Roering* et al., 1992a, b; *Perchuk* et al., 1996, 1999; *Mints* et al., 1996; *Perchuk* and *Krotov*, 1998; *Pozhilenko* et al., 1997) suggested that both low- and high-grade metamorphic rocks from these areas record evidence for metamorphic and tectonic events related to the thrusting of granulites onto the adjacent granite-greenstone terrains. In Southern Africa (the Limpopo Complex) and in the Kola Peninsula (the Lapland Complex) regional (crustal-scale) shear zones separate the granulite terrains from the lower grade granite-greenstone terrains. The

emplacement of relatively hot and ductile granulites onto relatively cold and brittle cratonic successions caused heat transfer from the exhuming granulites toward the underthrusted wall rocks, resulting in the development of dynamic polythermal-polybaric metamorphic zoning in the greenstone wall rocks (*Perchuk* et al., 1996; *Roering* et al., 1992a; *Perchuk* and *Krotov*, 1998).

Published data (e.g. *Kusnetsov*, 1941, 1988; *Kovrigina*, 1973, 1977; *Nozkhin*, 1983, 1985; *Gerya* et al., 1986; *Perchuk* et al., 1989; *Dacenko*, 1995) suggest that the Southern Yenisey Range of Eastern Siberia is composed of metamorphic complexes of different metamorphic grade separated by regional thrusts, traditionally interpreted as an accreted terrain (e.g. *Kovrigina*, 1973, 1977; *Dacenko*, 1995). The degree of metamorphism generally increases across the thrust system from greenschist and epidote-amphibolite facies conditions through amphibolite to granulite facies conditions (e.g. *Kusnetsov*, 1941, 1988; *Gerya* et al., 1986; *Perchuk* et al., 1989). However, the structural and metamorphic characteristics of the different complexes of the Southern Yenisey Range have not been studied in detail. We aim to demonstrate, based on detail structural and petrological studies, that the tectono-metamorphic pattern and geological evolution of the Southern Yenisey Range are in many respects similar to that of the Limpopo and Lapland terrains and are therefore probably also controlled by the process of exhumation of the granulite-facies rocks.

Geological setting of the Southern Yenisey Range

The Yenisey Range is situated in the major Baikalide Belt which subdivides Siberia into Western and Eastern Platforms. The Baikalide belt occurs as a semi-circular rim around the Eastern Siberian Platform that, among other geological features, also hosts the Yenisey Range (Fig. 1a). The Yenisey Range is about 700 km in length and 150 km wide and consists of metamorphic, magmatic and sedimentary complexes Archaean to Cenozoic in age (Fig. 1a).

The Southern Yenisey Range (Fig. 1b) constitutes an early Precambrian metamorphic terrain with an exposed outcrop length of about 200 km and a width of 50–70 km. The Range was subdivided, on the basis of metamorphic, petrological and geochemical evidence, into the Kanskiy-, Yeniseyskiy-, and Yukseevskiy Complexes (*Kusnetsov*, 1941, 1988; *Nozkhin*, 1983, 1985; *Gerya* et al., 1986; *Perchuk* et al., 1989). Published data (e.g. *Gerya* et al., 1986; *Perchuk* et al., 1989) suggested an increase in the metamorphic grade from greenschist to epidote-amphibolite facies in the Yukseevskiy Complex through amphibolite facies in the Yeniseyskiy Complex to granulite facies in the Kanskiy Complex (Fig. 1b). However, a comprehensive metamorphic database only existed for granulites of the Kanskiy Complex (*Perchuk* et al., 1989) while lower grade Yeniseyskiy and Yukseevskiy complexes were not studied in detail.

The regional structural framework of the Southern Yenisey Range was traditionally interpreted as a system of N-S to NW-SE oriented crustal blocks (Fig. 1b) composed of rocks of the Kanskiy, Yeniseyskiy and Yukseevskiy Complexes (e.g., *Kovrigina*, 1973, 1977; *Dacenko*, 1995). These blocks are internally characterized by large-scale (100–800 m) isoclinal folds dipping to the NE and accompanied by lineations and a regionally developed schistosity. Thrusts in the

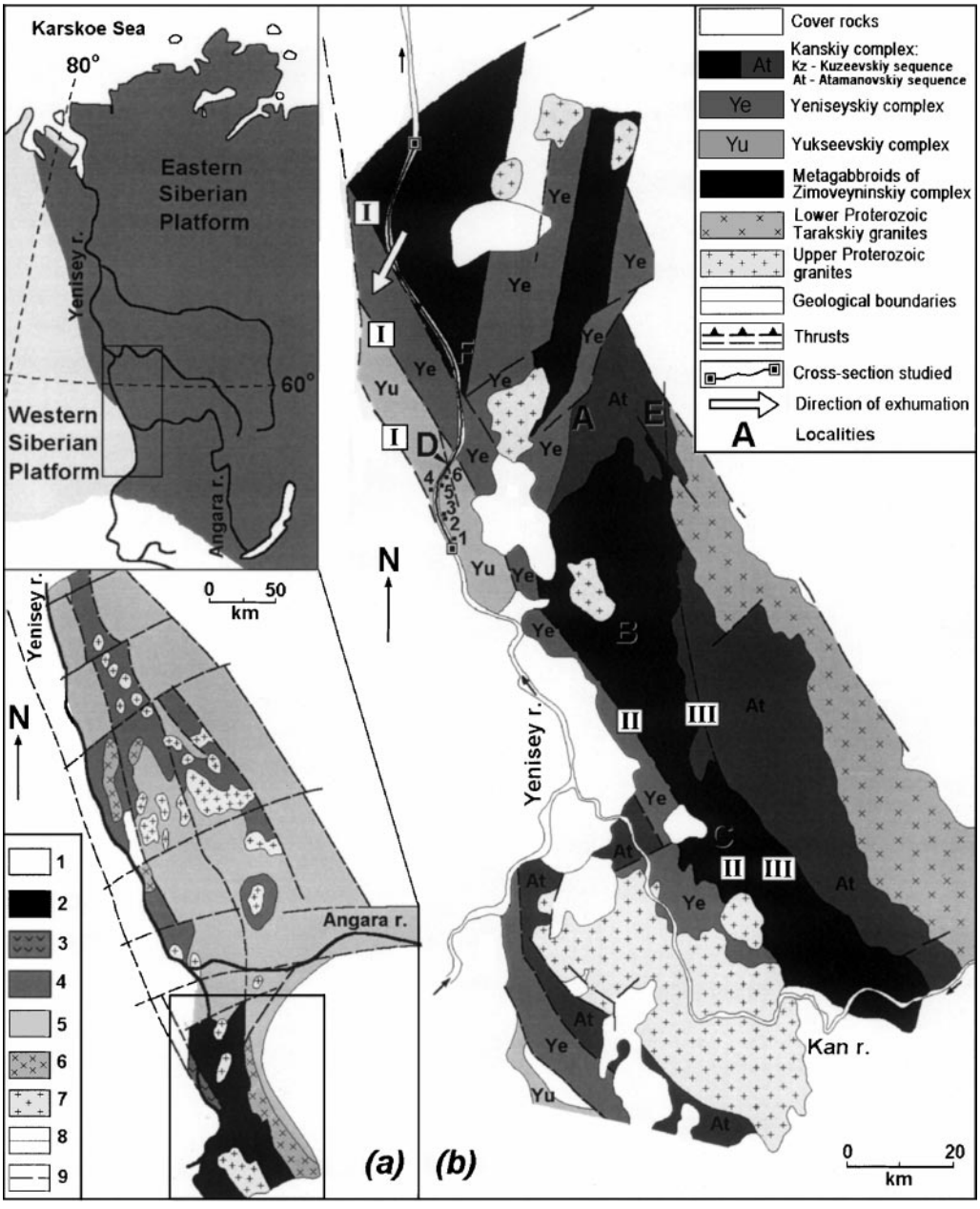

Fig. 1. Regional setting (**a**) and geological structure (**b**) of the Southern Yenisey Range, Eastern Siberia. **a** Main geological units of the Yenisey Range (*Gerya* et al., 1986). 1 = cover rocks; 2–4 = Pre-Riphean metamorphic complexes: 2 = Kanskiy and Yeniseyskiy granulite-gneissic complexes, amphibolite to granulite facies metamorphism (> 1900 Ma); 3 = Yukseevskiy greenstone complex, greenschists to epidote-amphibolite facies metamorphism (> 1900 Ma); 4 = Teyskiy complex (gneisses, carbonate rocks, quartzites, mica schists, metabasites), greenschists to amphibolite facies metamorphism (> 1650 Ma); 5 = Riphean volcanic and sedimentary complexes; 6 = Lower Proterozoic granitoids; 7 = Upper Proterozoic granitoids; 8 = geological boundaries; 9 = thrusts. **b** Geological map of the Southern Yenisey Range (*Gerya* et al., 1986; *Perchuk* et al., 1989; *Dacenko*, 1995; this study). Major regional thrust systems: I – Pri-Yeniseyskiy, II – Kansko-Posolnenskiy, III – Kansko-Shilkinskiy. Points with numbers show the location of samples listed in Table 1: 1 = T-5; 2 = T-218; 3 = T-233, T-235; 4 = T-244; 5 = T-255; 6 = T-42b, T-44a. A, B, C, D, E, F – specific localities referred in the text

area follow the general structural trend of the Range and three major regional thrust systems are distinguished from west to east in the Southern Yenisey Range (Fig. 1b): the Pri-Yeniseyskiy, Kansko-Posolnenskiy and Kansko-Shilkinskiy thrusts (*Kovrigina*, 1973). Their orientation changes from NW-SE in the south of the Range to N-S in the north, following the contours of the Siberian Craton. The thrust systems, which dip at 50–70 ° E to NE with a general vergence towards the west, are composed of up to 4 km wide zones of mylonitization and are characterized by the presence of magmatic complexes and hydrothermal ore deposits. This uniform structural pattern across the Southern Yenisey Range was traditionally attributed to folding during the systematic accretion of the Kanskiy, Yeniseyskiy and Yukseevskiy metamorphic Complexes onto the western boundary of the Eastern Siberian Craton (e.g. *Dacenko*, 1995). However, thrust kinematics across the complexes were not studied in detail.

The major stage of granulite facies metamorphism in the *Kanskiy Complex* was dated at 1800–2000 Ma., based on zircon studies (*Bibikova* et al., 1993; *Nozkhin* et al., 1989). This age correlates well with the emplacement age of the Tarakskiy granites (1900 $\pm$ 100 Ma, *Gerling* and *Artemov*, 1964; *Volobuev* et al., 1976). The dating also indicated an early thermal event restricted to the period 2650 $\pm$ 50 Ma (*Bibikova* et al., 1993; *Nozkhin* et al., 1989). The age of the protolith, however, exceeds 2700 Ma.

The major stage of epidote-amphibolite to amphibolite facies metamorphism in the *Yeniseyskiy Complex* (1900–1860 Ma, *Bibikova* et al., 1993; 1850 $\pm$ 150 Ma, *Nozkhin* et al., 1989) correlates with the main granulitic event in the Kanskiy Complex.

A wide range of zircon ages were determined for the rocks of the *Yukseevskiy Complex* (*Nozkhin* et al., 1989; *Nozkhin*, 1997): 2750 Ma, 1900 Ma, 1450 Ma, 1050 Ma, 870 Ma and 600 Ma. The 2750 Ma age is interpreted as the time of formation of the volcano-sedimentary protolith of the Yukseevskiy complex (*Nozkhin* et al., 1989). 1450 Ma stage corresponds to the formation of the regional sub-meridional tectonic structure (Fig. 1a) of entire Yenisey Range (*Nozkhin* et al., 1989). The three latest stages correlate with the ages of upper Proterozoic granites which intrude the Kanskiy Complex (*Volobuev* et al., 1976, 1980; *Dacenko*, 1984; *Nozkhin* et al., 1989).

The geochronology of the area is based on a very limited database but it does indicate that important metamorphic events in all three complexes of the Southern Yenisey Range occurred during the period 2000–1800 Ma. This period corresponds to the peak of the thermal activity in the area and with the formation of the Tarakskiy granitoid batholith during the final stages of granulite metamorphism.

Geology of the Yenisey River Section

Field work in the Southern Yenisey Range was executed during July 1997 along a 120 km section across the NW part of the area along the Yenisey River (Fig. 1b). The Range along this river section is deeply eroded, exposing the lithological, structural and metamorphic features of the Yukseevskiy, Yeniseyskiy and Kanskiy Complexes. The field study included detailed structural investigations ($>$ 500 structural measurements, $>$ 50 outcrop photographs) of different tectonic features

accompanied by systematic sampling (> 100 samples) of the cross section. In the field, the shear sense was deduced from σ- and δ-shaped winged porphyroclasts, small-scale folds, s-c relationships, mineral stretching lineations and other less abundant sense of movement indicators (e.g. *Simpson* and *Schmidt*, 1983; *Simpson*, 1986; *Passchier* and *Trouw*, 1996).

Representative samples of the different tectonites and metamorphic rocks were studied petrographically using 96 thin sections prepared from oriented samples. All thin sections were cut parallel to the kinematic plane. The most informative thin sections were also subjected to microprobe analyses (> 2000 analyses) using the scanning electron microscope (*CamScan-Cambridge*) of the Department of Petrology of Moscow State University equipped with an energy-disperse Link system. The structural and petrological data were used to investigate the metamorphic and tectonic history of the different complexes exposed along the river section.

Lithologies

Kanskiy Complex (formation). This granulite-facies complex is subdivided into a lower Kuseevskiy and an upper Atamanovskiy sequence (Fig. 1b). The Kuseevskiy sequence is mainly composed of *Grt-Pl*, *Grt-Opx-Pl* and *Opx-Pl*-gneisses and granulites, *Opx-Cpx-Pl* $\pm$ *Grt* metabasites, aluminous metapelites with *Grt*, *Crd*, *Sil*, *Spl* and *Opx* as well as some charnockites and enderbites. The sequence also contains several metagabbroid massifs of the Zimoveyninskiy Complex (Fig. 1b). The paragenesis *Qtz* + *Opx* + *Sil* that characterizes peak ($T \sim 900\,^{\circ}$C and $P \sim 8$ kbar) metamorphic assemblage is stable in some metapelites of the sequence (*Perchuk* et al., 1989). Maximal *P-T* conditions recorded in *Grt-Crd-Sil-Qtz* metapelites corresponds to $T = 795\,^{\circ}$C and $P = 6.1$ kbar (*Perchuk* et al., 1989). The Atamanovskiy sequence consists of aluminous *Grt-Bt*, *Grt-Crd-Bt*, *Grt-Crd-Sil-Spl* two-feldspar metapelites, *Opx-Grt-Bt*, *Opx-Bt-Crd* and *Opx-Pl* gneisses and rare *Opx-Cpx-Pl* metabasites. The paragenesis *Qtz* + *Opx* + *Sil* is not stable in metapelites of the sequence while maximal *P-T* conditions recorded in *Grt-Crd-Sil-Qtz* metapelites corresponds to $T = 716\,^{\circ}$C and $P = 4.5$ kbar (*Perchuk* et al., 1989). In the SE part of the area near the Tarakskiy pluton (locality E in Fig. 1b) some metapelites of the Atamanovskiy sequence contain andalusite (*Serenko*, 1969; *Perchuk* et al., 1989). The intensively migmatized northeastern portion of the sequence demonstrate a gradual transition into granites of the Tarakskiy pluton (*Dacenko*, 1984).

Metapelites from both sequences of the Kanskiy complex show near-isobaric cooling reaction textures such as replacement of cordierite by garnet, sillimanite and quartz (*Perchuk* et al., 1989). This textures are more characteristic for metapelites taken from areas farthest from Tarakskiy pluton and closest to the contacts between the Kanskiy and the Yeniseyskiy complexes (localities A, B, and C in Fig. 1b) (*Perchuk* et al., 1989). In the western part of the area close to Yenisey river this contact is also marked by appearance of *Opx* + *Sil* in metapelites (e.g. localities A and B in Fig. 1b) and *Opx* + *Cpx* + *Grt* + *Pl* in metabasites (e.g. locallities A, B and F in Fig. 1b) of the Kuseevskaya sequence (*Serenko*, 1969; *Perchuk* et al., 1989).

In spite of its high-grade character, the major rock types of the Kanskiy Complex are geochemically and petrochemically very similar to that of the

adjacent Yeniseyskiy and Yukseevskiy Complexes (*Nozkhin* and *Turkina*, 1993): the *Grt-Opx-Bt* gneisses are analogous with volcanic rocks of andesitic and dacitic compositions while the aluminose gneisses are similar to sedimentary pelitic rocks. *The Opx-Cpx-Pl* metabasites demonstrate characteristics of tholeiitic basalts. The average chemical composition of the Kanskiy Complex corresponds to that of diorite (*Perchuk* et al., 1989). An increase in the relative amount of mafic rocks in NW direction within the Kanskiy Complex was described by *Nozkhin* and *Turkina* (1993): along the Yenisey River a most significant amount of granulite-grade metabasic rocks is concentrated, including the 1.5×25 km layered Zimoveyninskiy metagabbroid massif (Fig. 1b).

Yeniseyskiy Complex (formation). This complex consists of epidote-amphibolite and amphibolite-facies rocks subdivided into a lower Isayevskiy and upper Srednyanskiy sequence. The rocks are migmatized and contain significant amounts of porphyroblastic and aplitic granites and pegmatites. Both sequences are mainly composed of *Bt-Pl*, *Grt-Bt*, *Hbl-Bt* and *Ms-Bt* gneisses and schists. In the lower portion of the formation amphibolites (metabasites) and acid metavolcanic rocks also occur. The upper portion is characterized by interlayered dolomitic and calcitic marbles, leucocratic plagiogneisses and sillimanitic gneisses, while the top of the formation is mainly composed of *Ms-Bt-Fsp-Qts* gneisses, marbles and quartzitic schists.

Yukseevskiy Complex (formation). This greenschist to epidote-amphibolite facies sedimentary-volcanic formation is subdivided into a lower Yudinskiy and upper Predivinskiy sequence. The complex is mainly composed of amphibolites, *Pl*-amphibolites (metabasites, metagabbroids), garnet-bearing *Pl-Qtz* rocks (acid metavolcanics) and less prominent *Hbl-* and *Bt-Hbl* schists and gneisses, *Grt*-bearing *Bt-Qtz* schists, quartzites, ferric quartzites, serpentinites, *Sil*-bearing *Bt*-schists as well as veins of deformed gneissic granites, aplites and pegmatites. By comparison to the Yeniseyskiy Complex the Yukseevskiy Complex contains abundant basic layers and shows systematically lower grade of metamorphism. The rock association (e.g. ferric quartzites, basic and ultrabasic rocks) and petrochemical and geochemical characteristics of the Yukseevskiy Complex are analogous to those of Archaean greenstone belts (*Nozkhin*, 1985).

Major tectonic events

The Southern Yenisey Range was affected by three related tectonic events. Each event is characterized by a specific group of tectonites:

(i) D1 gneisses, schists and metabasites from unsheared blocks (e.g. Fig. 2a, b);
(ii) D2 fault rocks, consisting both of mylonites (e.g. Fig. 2c, 3d) and straight gneisses (*Smit* and *Van Reenen*, 1997) and Fig. 2d, 3e.
(iii) D3 mylonites (e.g. Fig. 3a).

D1 fabric forming event. The early D1 foliation (S1) dominates the western part of the Southern Yenisey Range and is therefore well-developed in both the Yukseevskiy- (Fig. 2a) and in parts of the Yeniseyskiy Complex.

D1-gneisses (e.g. metadacites) and D1-mica schists of the *Yukseevskiy Complex* are characterized by well developed schists (Fig. 2a) with average grain size

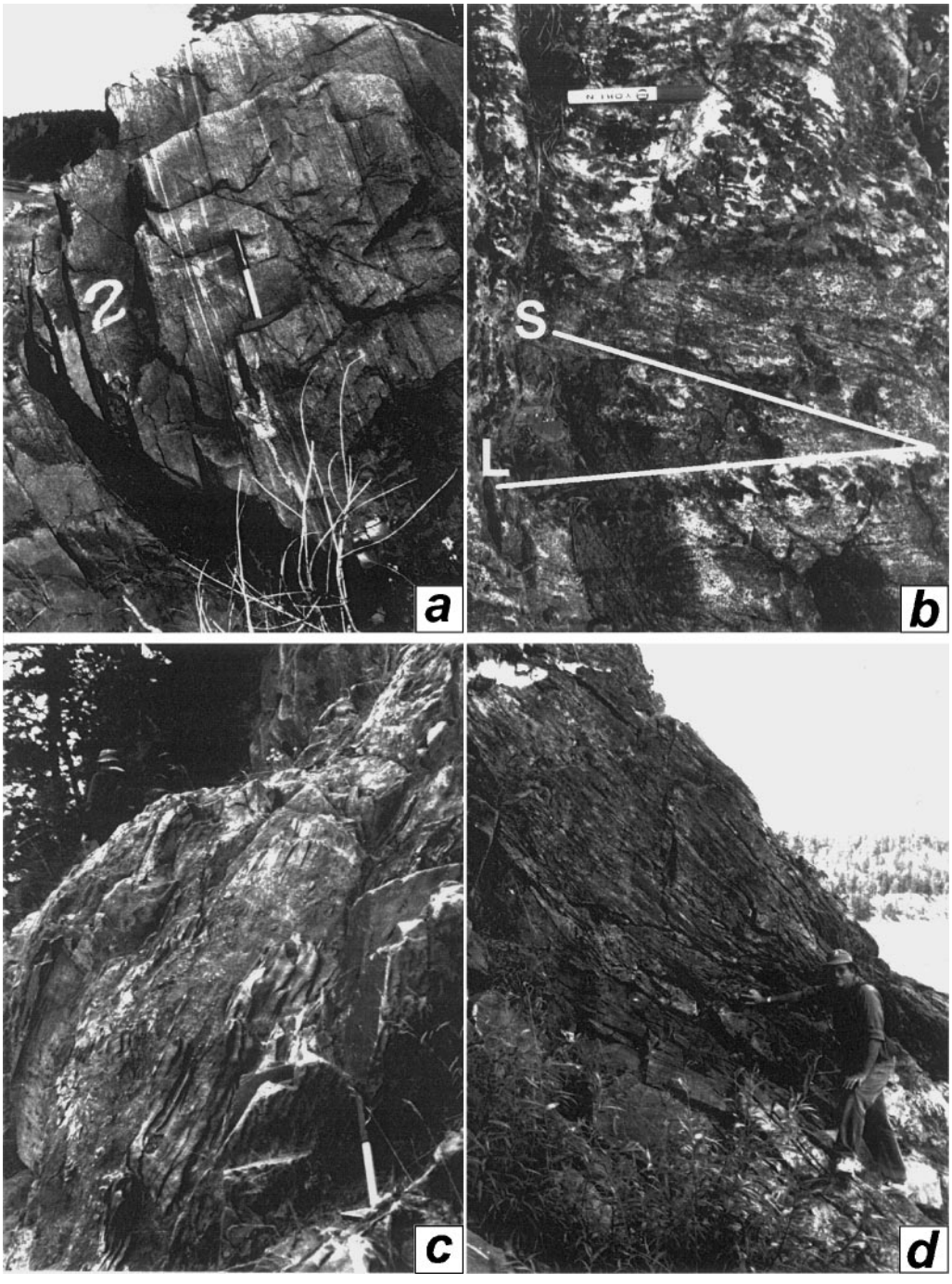

Fig. 2. Typical Dl and D2 structures developed in the metamorphic rocks of the studied complexes. **a** D1 fabric represented by S1 schistosity in the *Qtz-Pl-Bt*-gneiss of the Yukseevskiy complex. **b** Relationship of magmatic layering (L) and metamorphic S1 foliation (S) observed in the Zimoveyninskiy layered metagabbroid massif of the Kanskiy granulite complex. **c** D2 shear zone developed in metadacites of the Yukseevskiy Complex. Note the development of numerous steeply orientated small-scale sheath folds. **d** Straight gneiss of the Yeniseyskiy Complex from a regional D2 ductile shear zone situated at the transition of the Yeniseyskiy and Kanskiy Complexes. Note the consistent NE dip of the shear plane and the absence of folds. View towards the northwest

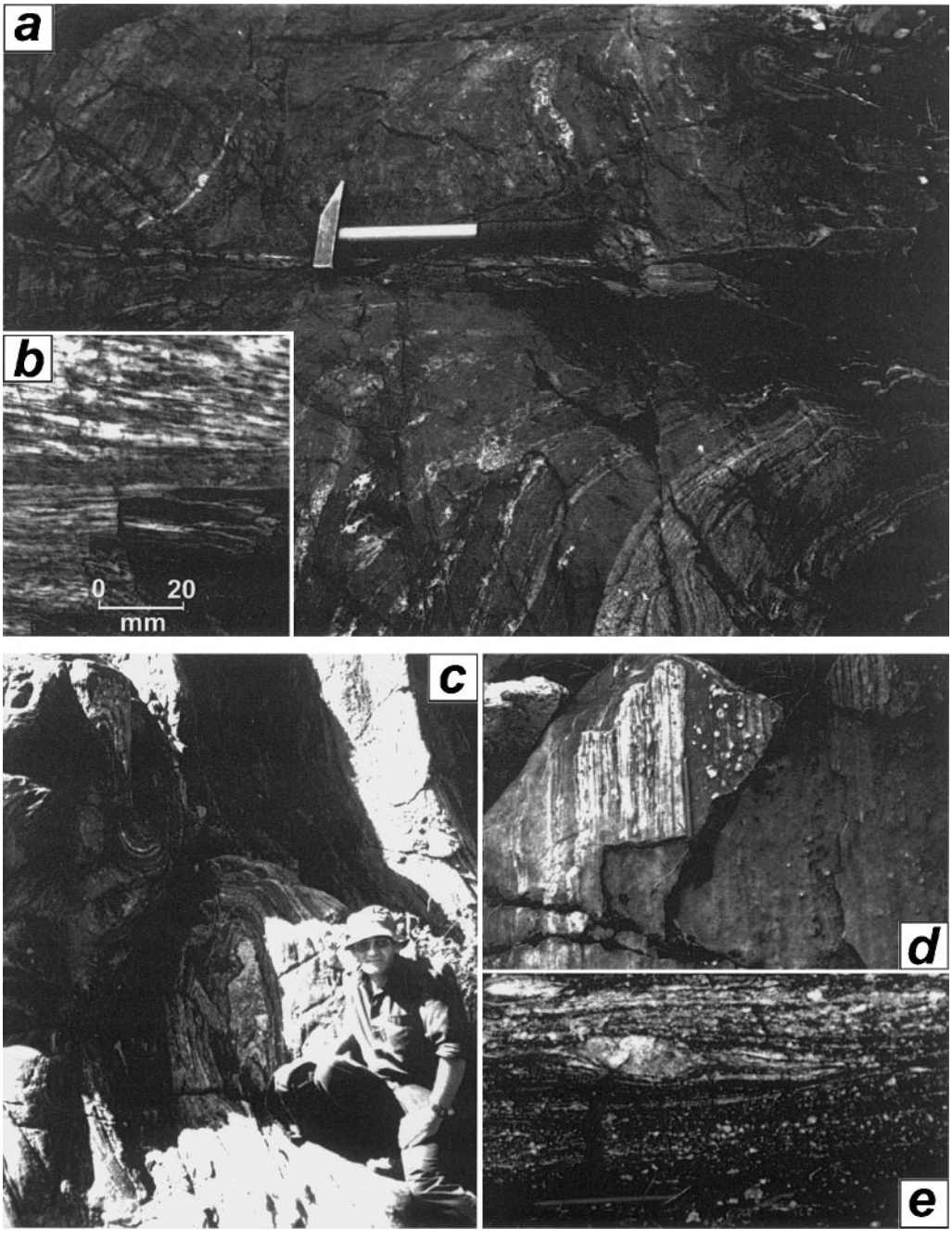

Fig. 3. Deformations of studied metamorphic rocks related to D2 and D3 events. **a** Small D3 mylonitic shear zone transposing the D2 fabric in metabasites of the Yukseevskiy Complex. **b** Close-up of the D3 mylonitic fabric in a metagabbroid of the Yukseevskiy Complex. **c** D2 folds with horizontal fold axis developed in rocks of the Yukseevskiy Complex. Note the axial-planar relationship with the D2 shear fabric. **d** D2 shear fabric developed co-planar to the S1 foliation and accompanied by down-dip mineral stretching lineations in metadacites of the Yukseevskiy Complex. **e** D2 straight gneiss fabric developed in *Bt-Hbl-Pl-Qtz* gneiss of the Yeniseyskiy Complex

0.02–0.1 mm. Porphyroblasts (0.1–1 mm) of *Grt* and *Pl* with clear pressure shadows can be observed. D1-metabasites are characterized by foliated lens-like structures with porphyroblasts (0.5–5 mm) represented by *Hbl*. The symmetric lens-like microstructures of D1-rocks are, however, characterized by the absence of clear sense of shear indicators and probably conform to a process of pure shear flattening.

D1-rocks in the *Yeniseyskiy Complex* are often preserved as unsheared 1–100 m lens-like fragments and boudins. Such rocks are characterized by either foliated granoblastic (*Bt-Hbl* gneisses and metabasites) or schistose porphyroblastic (*Grt*-bearing mica schists) microstructures. The average grain-size of the matrix minerals is 0.1–0.5 mm, i.e. generally larger than observed in the Yukseevskiy Complex.

D1-gneisses and metabasites in the *Kanskiy Complex* are characteristic of the inner part of the Complex. Close to its western boundary such rocks occur as separate lens-like blocks (thrust sheets) separated by younger D2 shear zones. These rocks are represented by medium- to coarse-grained granulites in which the foliation is defined by the orientation of elongated lens-like aggregates of *Opx* and *Grt*. In the Yenisey River section these rocks are well preserved within the Zimoveyninsky layered metagabbroid massif (Fig. 1b) in which the metamorphic foliation is superimposed (cross-cutting at 10–30°) on the initial magmatic layering (Fig. 2b).

D2 shear and folding event. The early S1 fabric in the lower grade Yukseevskiy complex is overprinted by discrete, up to 100 m wide ductile shear zones. The shear zones are composed of fine-grained mylonites (Fig. 2c, 3d) while further towards the east in the higher-grade Yeniseyskiy and Kanskiy Complexes these zones are commonly composed of medium grained straight gneisses (e.g. Fig. 4e). Another very prominent D2 feature of all the complexes is a system of tight to isoclinal meso- to large-scale folds (Fig. 3c) that accompany larger shear zones. These folds are relatively scarce in the Yukseevskiy and Yeniseyskiy Complexes but occur in abundance as isoclinal folds in the Kanskiy Complex. Both D2 folding and shearing become more prominent towards the east and finally culminate in a major ductile shear zone along the Yenisey/Kanskiy boundary (Fig. 2d).

D2-rocks are very common in the *Yukseevskiy complex*, especially in the eastern part, close to the boundary with the Yeniseyskiy Complex. Both acid and basic rocks of this type are characterized by asymmetric lens-like schistose porphyroblastic microstructures typical of an angular shear strain environment. In the mica schists very characteristic sigmoidal shaped micas can be observed. In some metadacites sigmoidal garnet and feldspar porphyroclasts occur. D2 shearing is also associated with mineral growth (e.g. rotated *Grt* porphyroblasts) and does not normally lead to classic grain-size reduction of the matrix minerals. The average size of the matrix minerals (0.02–0.1 mm) therefore do not differ from those in D1 rocks.

In the *Yeniseyskiy complex* D2-rocks are especially well developed in the eastern part close to the boundary with the granulite facies Kanskiy Complex (Fig. 2d) and occur in a tectonic melange zone that contains large (up to 100 m) lens-like boudins of massif metabasites enveloped by sheared rocks suggesting intensive displacement of the lithologies during D2 shear event. D2-rocks are represented by medium grained straight gneisses (*Smit* and *Van Reenen*, 1997) and metabasites

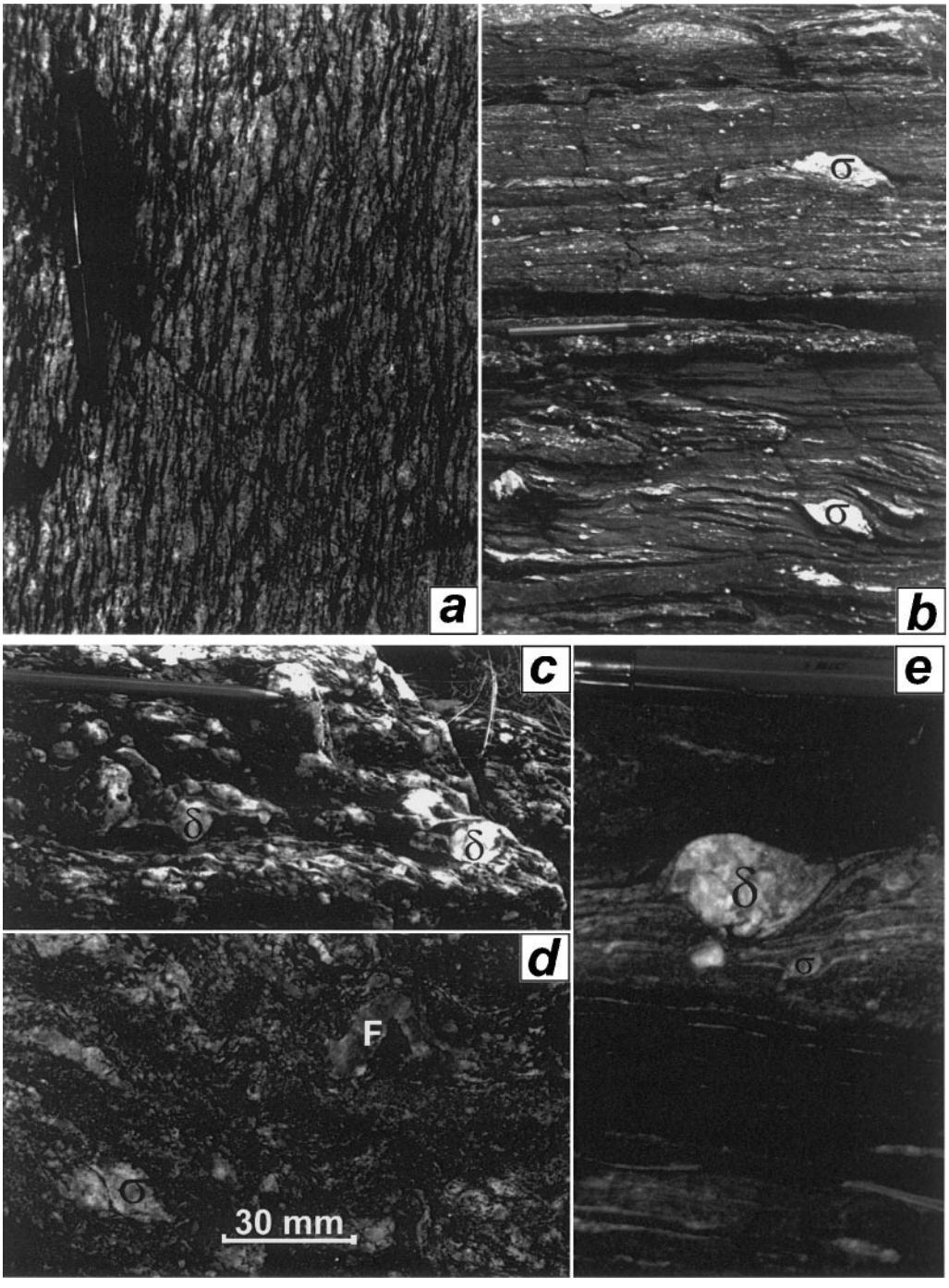

Fig. 4. Close-up of D1 and D2 fabrics in the studied metamorphic rocks. **a** Symmetric lens-like schistose D1 fabric of *Qtz-Pl-Bt*-gneiss of the Yukseevskiy complex. **b** Strongly sheared gneisses of the Yeniseyskiy Complex from a large-scale ductile shear zone (Fig. 2c) situated at the transition of the Yeniseyskiy and Kanskiy Complexes. σ-type winged porphyroblasts of feldspars indicate sinistral shear movement. View towards the west. **c**, **d**, **e** Shear sense indicators in gneisses of the Yeniseyskiy Complex. Symbols denote microfolds (F), σ- and δ-type winged porphyroblasts of feldspars indicate sinistral (**c**, **d**) and dextral (**e**) shear movement

with clear mineral stretching lineations. Abundant sense of shear indicators (Fig. 4b, c, d, e) are represented by rotated porphyroblasts (1–20 mm) of *Pl* and *Kfs*. D2 shearing is associated with mineral growth (e.g. rotated porphyroblasts) and do not normally lead to grain-size reduction of the matrix minerals. The average size of matrix minerals (0.1– 0.5 mm) is similar to that of D1 rocks.

D2-straight gneisses and mylonites are abundant in the Kanskiy Complex close to its sheared boundary with the Yeniseyskiy Complex. They are represented by dry and hydrated sheared granulites characterized by grain-size reduction (0.02–0.1 mm), medium and fine-grained quartz ribbons and brittle deformation of early garnet porphyroblasts. Abundant sense of shear indicators are represented by sigmoid shaped porphyroblasts of *Grt* (1–7 mm) and *Qtz* (1–5 mm) surrounded by mylonitized matrix minerals. A clear shift of small (0.05–0.1 mm) *Grt* fragments with the transport direction can be observed in the wings of porphyroblasts. In several cases mylonitization is associated with the replacement of *Grt* by *Bt*. Quartz, plagioclase and biotite demonstrate a ductile style of deformation. Very specific mylonites that formed after metagabbroids occur close to the western contact of the Zimoveyninskiy massif (locality F in Fig. 1b). In these mylonites ductile deformation of early coarse grained (1–10 mm) *Pl* and *Opx* is associated with the development of syntectonic fine-grained (0.02–0.05 mm) *Pl* ribbons and of *Grt-Cpx-Qtz* coronitic textures around *Opx*. The appearance of small inclusions of *Spl* in early *Pl* also occur. This suggests the crystallization of a new paragenesis in the reaction $Opx + Pl \Rightarrow Grt + Qtz + Cpx$ during the D2-shearing process that occurred at relatively high *P-T* conditions. Such relationships are typical for the so called ≪primary straight gneisses≫ (*Smit* and *Van Reenen*, 1997) that represent shear processes at lower crustal levels.

D3 shear event. Younger mylonitic shear zones (Fig. 3a) were observed throughout the mapping area. They mainly developed under greenschists facies conditions and clearly affected D2 shear zones. Large up to 300 m wide D3 shear zones occur in the Yukseevskiy complex close to its boundary with the Yeniseyskiy complex (locality D in Fig. 1b).

D3 rocks of the *Yukseevskiy Complex* are classical mylonites characterized by significant grain-size reduction (< 0.01 mm) of the matrix minerals and by abundant greenschists facies minerals (chlorite, actinolite, sericite, carbonates) replacing early epidote-amphibolite facies parageneses. In most mylonites s-c angles are close to 0° indicating large gamma values. Sense of shear indicators are represented by sigmoid shaped winged *Pl* porphyroclasts with wings composed of carbonates.

In the *Yeniseyskiy Complex* the D3-mylonites are very abundant along the boundary with the Yukseevskiy Complex. Microstructures in these mylonites are best preserved in *Grt*-bearing rocks where garnet porphyroblasts (1–10 mm) are partially destroyed by intense mylonitization. The mylonites are characterized by subparallel s-c surfaces and significant grain-size reduction (0.01–0.02 mm) similar to that observed in D2 gneisses of Yukseevskiy Complex (but still larger than D3-mylonites of Yukseevskiy Complex). Sense of shear indicators are widely represented by sigmoidal-shaped *Grt* porphyroblasts with wings mainly composed of *Bt*. In some cases a clear shift of small (0.05–0.1 mm) *Grt* fragments with the transport direction can be observed in the wings of the porphyroblasts. The latest

stage of this process is characterized by the replacement of *Grt* along cracks by post-D3 generations of *Bt*, *Ms* and *Chl*. Similar replacements can also be observed in non-mylonitized D1-gneisses of the Yeniseyskiy Complex close to its western boundary.

D3 mylonites in the *Kanskiy Complex* are not intensely developed and occur as narrow (10 m) zones that formed under epidote-amphibolite to greenschists facies conditions of metamorphism.

Kinematics of the Southern Yenisey Range

The study of different tectonic indicators (e.g. Fig. 4) has shown that in each of three complexes tectonic fabric corresponding to subsequent D1, D2 and D3 events are co-planar but clearly angular with respect to their sense of movement.

Yukseevskiy Complex. In the western portion of the Yukseevskiy Complex the S1 fabric that trends in a general NNW direction and dipping at steep angles to both the WSW and ENE probably represents pre-D2 regional fabric of the Southern Yenisey Range (Fig. 5a). D1 fabric is sporadically overprinted by a younger D2-shear fabric or by discrete younger D2-shear zones. Abundant movement indicators suggest top to the WNW D2 thrust movement (Fig. 5a). Meso- to large-scale folds accompanying the D2 shear zones are characterized by near-horizontal fold axes that develop axial planar to the D2 shear fabric (Fig. 5a). The folds are observed in outcrop (Fig. 3c) but can also be deduced from the fact that S1 dips steeply to both the west and east conforming to re-folding (Fig. 5a). Observed pattern of D2 shear zones and folds is consistent with the SW-NE contractional system. D3 mylonitic shear zones developed in the Yukseevskiy complex (Fig. 5a) are also WNW-striking near vertical fault planes. These shear zones, however, are characterized by near horizontal mineral stretching lineations with dextral strike-slip movement (Fig. 3b, 5a).

Yeniseyskiy Complex. Orientation of the regional D1 fabric in the Yeniseyskiy Complex is almost identical to that of the adjacent Yukseevskiy Complex (compare Fig's 5a, b). The D1 fabric still trends almost N-S dipping at steep angles towards both the WSW and ENE, again indicating large-scale D2 folding that in this case, becomes a dominant meso-scale feature. These D2 folds again refold the regional D1 fabric suggesting that the same contractional forces operative in the Yukseevskiy Complex also affected these rocks (Fig. 5b). The semi-parallel D2 shear zones become more prominent towards the Yeniseyskiy/Kanskiy contact zone where all older structural features are almost completely obliterated (Fig. 2d, 4b). D3-mylonitization in the Yeniseyskiy Complex results in intense transposition of D1 and D2 structural elements into the D3 shear direction (Fig. 5b). The three tectonic fabrics are again co-planer but angular with respect to their sense of movement (NNW thrust sense for D2 and N-S dextral strike-slip movement for D3).

Yeniseyskiy/Kanskiy complexes boundary (regional D2 shear zone). Towards the Yeniseyskiy/Kanskiy contact the geometrical pattern of thrust movement changes dramatically. Near the contact the plane of deformation also significantly changes from a folded N-S trending fabric in the Yeniseykiy proper (Fig. 5b, c) to a NW-trending fabric that consistently dips at a shallow (45°) angle towards the NE

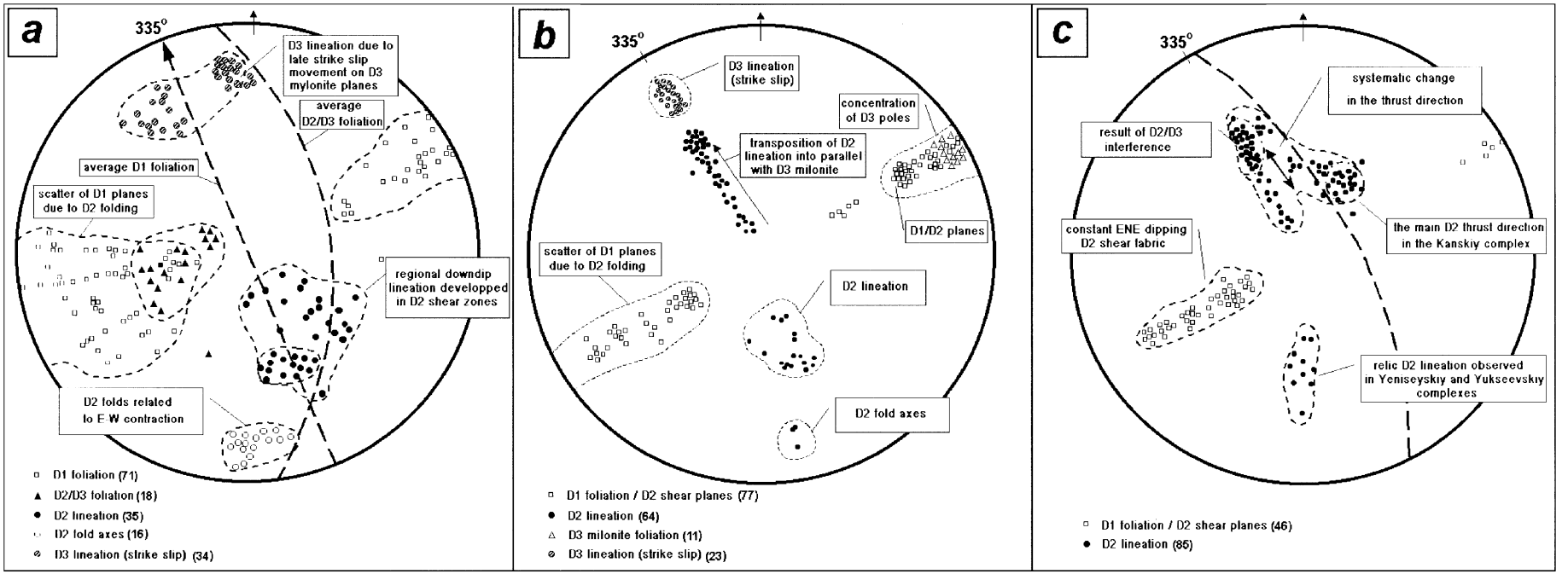

Fig. 5. Equal area plots of structural elements measured in rocks of the Southern Yenisey range. **a** Yukseevskiy Complex including the Yukseevskiy/Yeniseyskiy Complex boundary; **b** Yeniseyskiy Complex with mylonite belts; **c** Kanskiy Complex including the Yeniseyskiy/Kanskiy Complex boundary

(Fig. 2d). In this transition zone the structural geometry is that of an imbricate thrust stack with transport towards the SW. Relict D2 lineation elements representing D2 fold axis and D2 lineations are still present (compare Figs. 5b, c). The dominant D2 shear fabric now shows very little evidence for folding and dips at a constant angle to the ENE parallel to the crustal scale shear zone at the contact between the Yeniseyskiy and Kanskiy Complexes (Fig. 2d). A different but very dominant lineation appears within this transitional area that represents the major SW thrust event. This indicates that the D2 transport direction observed in both the Yukseevskiy and Yeniseyskiy proper (Fig. 5a, b) changes at this contact zone with the Kanskiy Complex to a more SW-directed thrust movement (Fig. 5c). Two important structural features of regional D2 shear zone at the Yeniseyskiy/ Kanskiy contact should be underlined:

(i) The steep and strongly folded D1 fabric that dominates the Yukseevskiy and Yeniseyskiy Complexes (Fig. 2a, 5a, b) changes into a shallow NE dipping fabric (Fig. 2d, 5c); even the isocinal folds become low-angles structures.
(ii) The steeply SE dipping D2 shear lineation in the Yukseevskiy and Yeniseyskiy Complexes (Fig. 5a, b) changes in orientation to a steeply NE dipping shear lineation (Fig. 5c).

Kanskiy complex. Structural data from the Kanskiy Complex proper (Fig. 5c) suggest that the structural elements that characterize this granulite terrain are consistent with the SW-NE contractional system suggested for D2 structures in both the Yeniseyskiy and Yukseevskiy Complexes. Shear sense indicators are unequivocal, suggesting thrusting of the granulites onto the rocks of Yeniseyskiy Complex along the SW verging bounding shear zone. The geometry of abundant D2 isoclinal folds are parallel with those observed in the other two complexes (compare Fig. 5a, b, c).

Mineralogy and petrology

Regional variations

During the present investigation a general increase in the grade of metamorphism was observed from the SW to the NE across the study area. Within this cross section the amount of garnet-bearing rocks statistically increases from only a few varieties in the Yukseevskiy Complex to numerous garnet-bearing gneisses and metabasites in the Yeniseyskiy and Kanskiy Complexes. A regular change in the paragenesis of metabasites can also be distinguished. While metabasites of the Yukseevskiy Complex mainly contain the paragenesis $Hbl + Pl + Ep$ without garnet the association $Hbl + Pl + Cpx + Grt$ is very common in the Yeniseyskiy Complex while in the Kanskiy Complex metabasites are mainly represented by *Opx-Cpx-Pl-Grt* and *Opx-Cpx-Pl* varieties with hornblende mainly developed as a retrograde phase. Compositions and bulk Mg numbers of metabasites of all three complexes (*Gerya* et al., 1986) are quite similar: Kanskiy Complex–$N_{Mg} = 27$–71 (mean value–49), Yeniseyskiy complex–$N_{Mg} = 26$–66 (mean value–49), Yukseevskiy complex–$N_{Mg} = 34 - 70$ (mean value–49). Therefore, observed changes in mineral assemblages should be mainly attributed to the systematic increase in metamorphic conditions.

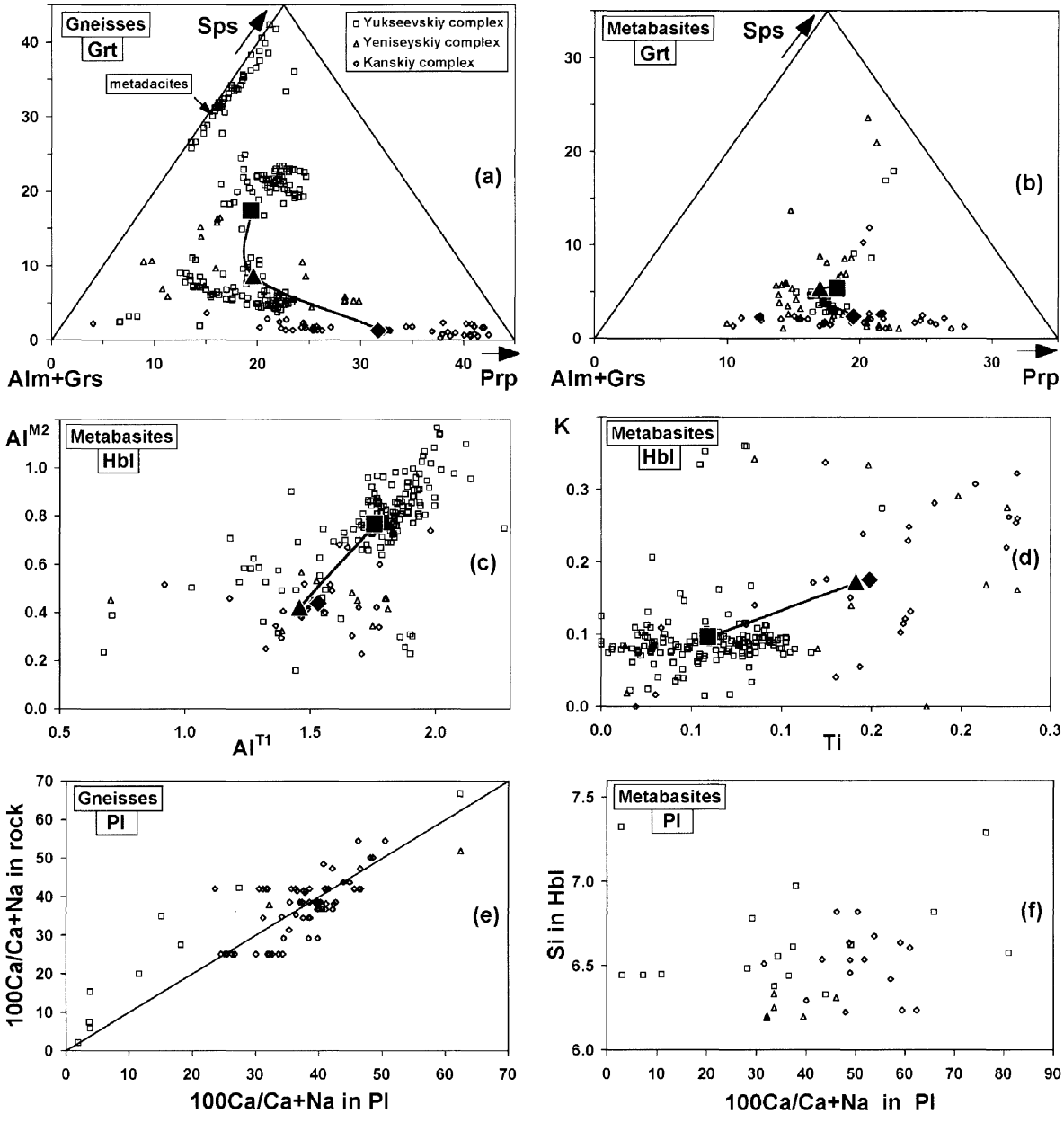

Fig. 6. Regional variation in the composition of garnet (**a**, **b**), hornblende (**c**, **d**) and plagioclase (**e**, **f**) in gneisses and schists (**a**, **e**) and metabasites (**b**, **c**, **d**, **f**) from the studied cross-section. Large solid symbols along the trends (**a**, **b**, **c**, **d**) show calculated average compositions of garnet in (**a**, **b**) and hornblende (**c**, **d**) for the corresponding complexes

The increase in the degree of metamorphism correlates with changes in composition of rock-forming minerals. The diagrams (a) and (b) of Fig. 6 represent the compositions of garnet analyzed in gneisses and schists (Fig. 6a) and in metabasites (Fig. 6b) for all three complexes. The change in average garnet composition for both gneisses (Fig. 6a) and metabasites (Fig. 6b) reflects a

Table 1. *Mineral assemblages of representative samples of D2-sheared rocks of the Yukseevskiy complex*

Sample	Rock	Mineral assemblage
T-5	Meta-andesito-dacite	$Qtz_{B,C}^{*}(60\%) + Pl_{B,C}(20\%) + Grt_{B,C}(15\%) + Hbl_{B,C}(5\%) + Chl_{C}(<1\%) + Bt_{B,C}(<1\%) + Ep_{B,C}(<1\%)$
T-218	Mica schist	$Pl_{B,C}(35\%) + Bt_{B,C}(30\%) + Qtz_{B,C}(20\%) + Ms_{B,C}(7\%) + Mag_{B,C}(5\%) + Grt_{C}(3\%) + Ep_{B,C}(<1\%)$
T-233	Garnet-bearing amphibolite	$Hbl_{B,C}(70\%) + Pl_{B,C}(10\%) + Ep_{B,C}(10\%) + Qtz_{B,C}(5\%) + Grt_{C}(4\%) + Chl_{C}(1\%)$
T-235	Gneiss	$Qtz_{B,C}(35\%) + Hbl_{B,C}(20\%) + Grt_{A,B,C}(15\%) + Bt_{B,C}(10\%) + Pl_{B,C}(10\%) + Ep_{B,C}(3\%) + Chl_{C}(7\%) + Mag_{B,C}(<1\%)$
T-244	Porphyroblastic amphibolite	$Hbl_{B,C}(60\%) + Pl_{B,C}(15\%) + Qtz_{B,C}(10\%) + Ep_{B,C}(10\%) + Chl_{C}(5\%) + Mag_{B,C}(<1\%)$
T-255	Mica schist	$Qtz_{B,C}(40\%) + Bt_{B,C}(30\%) + Pl_{B,C}(15\%) + Grt_{C}(10\%) + Ep_{B,C}(5\%) + Mag_{B,C}(<1\%)$
T-42b	Gneiss	$Bt_{B,C}(25\%) + Pl_{B,C}(25\%) + Qtz_{B,C}(15\%) + Hbl_{B,C}(15\%) + Chl_{C}(10\%) + Grt_{C}(7\%) + Ep_{B,C}(3\%)$
T-44a	Metadacite	$Qtz_{B,C}(70\%) + Bt_{B,C}(20\%) + Grt_{A,B,C}(7\%) + Ms_{B,C}(2\%) + Pl_{B,C}(1\%) + Mag_{B,C}(<1\%) + Ep_{B,C}(<1\%)$

*detected structural generations of the mineral (see text): *A* pre-D2 (syn-D1), *B* Syn-D2, *C* post-D2

statistical decrease in *Sps*, *Grs* and an increase in the *Prp* content from Yukseevskiy toward the Yeniseyskiy and Kanskiy complexes. The lowest Mg contents ($N_{Mg} = 0.5$–1.5) were analyzed in garnets of massive and gneissic metadacites of the Yukseevskiy Complex (T-44a, Table 1) due to the very low Mg/Fe ratio of the rocks ($N_{Mg} = 0$–17, mean value 7.4). Garnet very rich in *Grs* and *Sps* clearly forms separate fields on the diagram of Fig. 6a and are associated with Mg-poor *Bt* ($N_{Mg} = 7$).

The difference in the conditions of metamorphism also correlates with changes in the compositions of amphibole analyzed in metabasites of all three complexes (Fig. 6c, d). The average composition of hornblende of the Yukseevskiy Complex differ significantly from that of the Kanskiy and Yeniseyskiy Complexes due to higher Al^{M2} (Fig. 6c) and lower K and Ti (Fig. 6d) contents.

Plagioclase is stable in all types of silicate rocks of all three complexes. Diagrams (e) and (f) of Fig. 6 represent *An* contents in plagioclase analyzed in gneisses (Fig. 6e) and in metabasites (Fig. 6f). Variations of *Pl* compositions in gneisses (Fig. 6e) correlate with bulk Ca/(Ca + Na) ratio of the rocks while in metabasites there is no such correlation. By comparison to the Yeniseyskiy and Kanskiy complexes plagioclases from metabasites of the Yukseevskiy complex vary significantly (Fig. 6f) demonstrating both albite-rich ($N_{An} = 0$–10) and anorthite-rich ($N_{An} = 70$–80) compositions. *Ab*-rich plagioclases of metabasites are

probably formed at greenschists facies conditions are not systematically associated with actinolite-rich amphiboles (Fig. 6f). *An*-rich plagioclases presumably represent relic igneous compositions. In mica schists of the Yukseevskiy complex the composition of plagioclase varies from An_{30} to An_{40}.

The distribution of different mineral assemblages within the studied cross-section clearly reflect a dynamic (tectonic) input during the development of the rocks and do therefore not conform to a static thermal metamorphic zonation. The most significant changes in mineral parageneses and chemistry of the study area are restricted to the relatively narrow zones of intensive D2 shear deformations, especially where they occur at the boundaries of the different complexes.

Mineralogy and petrology of representative samples

The petrology, reaction textures and *P-T* conditions of metamorphism of the granulites of the Kanskiy Complex were studied in detail by *Perchuk* et al. (1989). The present study therefore mainly concentrated on the low-grade greenstone belt part of the cross-section as represented by data collected from the Yukseevskiy Complex. Among a large variety of metamorphic rocks occurring in this complex, the garnet-bearing gneisses and metabasites significantly affected by the D2 shear event were studied to determine the physico-chemical conditions of metamorphism. These rocks demonstrate clear tectonic micro-textures, allowing the determination of subsequent generations of minerals (e.g. *Gerya* et al., 1997). Combined microstructural, petrological, and microprobe studies were done for representative samples listed in Table 1. Selected microprobe analyses for the samples are given in Table 2.

Two major types of garnet, differing with reference to the shape of porphyroblasts, inclusions and chemical zoning, were found. The first (syn-D2) type is represented by large, up to 10 mm in diameter, garnet porphyroblasts with isometric or irregular forms that are mainly syn-tectonic relative to D2 shearing (Fig. 7a). These garnets were found in gneisses of andesitic (T-235) and dacitic (T-44a) composition. The porphyroblasts have clear pressure shadows and are characterized by isometric quarts inclusion trails oriented at an angle to the main schistosity. The inclusions also reflect some rotation of garnet during the D2 shear stage. The garnets are characterized by reversible chemical zoning (Fig. 8a, c), reflecting both the prograde and retrograde stages of metamorphism. The cores are characterized by low Mg and high Mn contents while the inner rims are relatively rich in Mg and poor in Mn. The narrow (0.05–0.1 mm) outer rims, however, demonstrate a decrease in *Prp* and sometimes an increase in the *Sps* and *Grs* content.

The second (post-D2) type of garnet is represented by irregular and isometric grains without pressure shadows that are late to post-tectonic relative to the main schistosity (shear planes), and therefore the D2 event (Fig. 7b). In the gneisses and schists (e.g. T-218, T-235, Table 1, 2) this garnet is mainly represented by small 0.1–0.5 mm inclusion-free grains while in garnet-bearing amphibolite it forms large, up to 7 mm porphyroblasts with inclusion-rich cores and inclusion-free rims (e.g. T-233, Table 1, 2). The composition of these garnets are identical to that of the outer rims of syn-D2 garnet. Chemical zoning of post-D2 garnet is characterized by

Table 2. *Representative microprobe analyses* of coexisting minerals from the samples studied*

Sample	T-42b	T-42b	T-42b	T-42b	T-218	T-218	T-218	T-218	T-218	T-218	T-233	T-233	T-233	T-233
Mineral	*Grt*	*Grt*	*Chl*	*Bt*	*Grt*	*Grt*	*Bt*	*Bt*	*Ms*	*Pl*	Grt	Grt	Hbl	Hbl
	core	rim	rim	core	core	rim	core	rim	rim	core	core	rim	core	rim
Generation	Post D2	Post D2	Post D2	Post D2	Post D2	Post D2	Post D2	Post D2	Post D2	Post D2	Post D2	Post D2	Post D2	Post D2
Spot	48	6	7	42	4.44	4.40	4.38	4.39	4.59	4.48	5.50	5.51	5.69	5.70
SiO_2	36.70	37.20	31.59	38.26	36.70	36.47	37.27	35.46	48.37	60.43	37.31	37.81	43.79	43.30
TiO_2	0.00	0.12	0.09	1.30	0.00	0.00	2.08	1.41	0.89	0.04	0.08	0.11	0.76	0.64
Al_2O_3	21.37	21.14	21.70	18.75	21.13	21.31	19.82	19.89	35.43	24.79	21.35	21.47	14.08	15.65
FeO	24.81	25.74	23.44	18.62	27.63	27.96	19.30	23.38	3.35	0.13	28.62	28.37	18.76	18.52
MnO	8.31	8.13	0.67	0.17	8.69	9.24	0.21	0.29	0.00	0.00	2.10	2.20	0.33	0.18
MgO	3.18	2.63	22.30	13.06	3.80	2.96	12.19	13.51	0.77	0.09	3.59	3.21	8.95	8.15
CaO	5.23	5.03	0.10	0.00	1.94	1.67	0.00	0.13	0.00	6.29	6.82	6.81	11.71	11.73
Na_2O	0.41	0.00	0.11	0.20	0.08	0.33	0.38	0.39	0.27	8.16	0.11	0.00	1.16	1.35
K_2O	0.00	0.00	0.01	9.65	0.04	0.07	8.76	5.55	10.92	0.08	0.00	0.02	0.47	0.41
Crystallographic formulas**														
Si	2.913	2.979	2.848	2.775	2.936	2.926	2.699	2.482	3.064	2.685	2.953	2.999	6.309	6.255
Ti	0.000	0.007	0.006	0.071	0.000	0.000	0.113	0.074	0.042	0.001	0.005	0.007	0.082	0.070
Al	1.999	1.994	2.305	1.603	1.993	2.015	1.691	1.640	2.644	1.297	1.991	2.006	2.390	2.665
Fe	1.646	1.723	1.766	1.129	1.848	1.876	1.169	1.368	0.177	0.005	1.893	1.881	2.259	2.236
Mn	0.558	0.551	0.051	0.010	0.589	0.628	0.013	0.017	0.000	0.000	0.140	0.148	0.041	0.022
Mg	0.376	0.314	2.995	1.412	0.453	0.353	1.315	1.409	0.072	0.006	0.423	0.379	1.920	1.753
Ca	0.444	0.432	0.009	0.000	0.166	0.144	0.000	0.010	0.000	0.299	0.578	0.578	1.807	1.814
Na	0.064	0.000	0.018	0.028	0.012	0.051	0.054	0.053	0.034	0.702	0.017	0.000	0.324	0.377
K	0.000	0.000	0.001	0.892	0.004	0.007	0.809	0.495	0.882	0.005	0.000	0.002	0.087	0.076
X_{Mg}	0.186	0.154	0.629	0.556	0.197	0.159	0.529	0.507	–	–	0.182	0.168	0.459	0.439

(continued)

Table 2 (*continued*)

Sample	T-244	T-244	T-244	T-244	T-235	T-235	T-235	T-235	T-235	T-235	T-235	T-235	T-255	T-255
Mineral	*Hbl*	*Hbl*	*Hbl*	*Hbl*	*Grt*	*Grt*	*Hbl*	*Hbl*	*Bt*	*Bt*	*Grt*	*Grt*	*Grt*	*Bt*
	core	rim	core	rim	core	rim	core	rim	core	rim	core	rim	core	core
Generation	Syn D2	Syn D2	Post D2	Post D2	Syn D2	Syn D2	Syn D2	Syn D2	Syn D2	Syn D2	Post D2	Post D2	Post D2	Post D2
Spot	2–7	2–32	5–37	5–42	6.11	4.16	5–6	5–5	3.18	4.12	9	13	44	54
SiO_2	44.08	42.75	44.05	48.25	36.82	37.91	43.37	41.92	38.01	37.26	37.30	36.92	37.31	38.92
TiO_2	0.55	0.57	0.96	0.43	0.04	0.19	0.59	0.50	1.70	1.70	0.00	0.00	0.07	1.88
Al_2O_3	15.19	16.63	15.53	11.02	21.10	21.44	15.61	16.70	19.27	19.80	21.41	21.01	20.94	18.20
FeO	13.60	13.70	13.31	11.60	28.72	29.80	18.43	19.87	21.04	21.89	29.88	32.11	20.61	19.73
MnO	0.29	0.22	0.35	0.26	5.39	2.45	0.25	0.17	0.00	0.10	2.18	3.46	10.38	0.34
MgO	11.88	11.30	11.41	14.29	3.46	3.67	8.38	7.33	10.77	10.56	5.01	2.75	3.33	12.33
CaO	12.00	12.13	12.24	12.45	4.24	4.21	11.05	11.33	0.00	0.13	3.83	3.59	7.27	0.11
Na_2O	1.89	2.18	1.58	1.45	0.23	0.31	1.90	1.83	0.04	0.00	0.40	0.16	0.06	0.20
K_2O	0.53	0.52	0.53	0.22	0.01	0.01	0.42	0.37	9.17	8.55	0.00	0.00	0.03	8.30
Crystallographic formulas**														
Si	6.249	6.090	6.260	6.762	2.933	3.006	6.244	6.079	2.783	2.713	2.935	2.962	2.956	2.807
Ti	0.059	0.061	0.102	0.046	0.002	0.011	0.064	0.055	0.093	0.093	0.000	0.000	0.004	0.102
Al	2.538	2.791	2.600	1.820	1.980	2.003	2.648	2.854	1.662	1.699	1.985	1.986	1.955	1.547
Fe	1.612	1.632	1.581	1.358	1.912	1.975	2.218	2.409	1.287	1.332	1.965	2.154	1.365	1.190
Mn	0.034	0.027	0.042	0.030	0.363	0.164	0.031	0.020	0.000	0.006	0.145	0.235	0.696	0.021
Mg	2.508	2.398	2.415	2.983	0.411	0.434	1.796	1.583	1.174	1.146	0.587	0.328	0.394	1.324
Ca	1.821	1.851	1.863	1.869	0.361	0.358	1.704	1.759	0.000	0.010	0.322	0.308	0.617	0.008
Na	0.518	0.601	0.436	0.395	0.036	0.048	0.529	0.514	0.005	0.000	0.061	0.025	0.009	0.028
K	0.095	0.095	0.096	0.039	0.001	0.001	0.077	0.068	0.856	0.794	0.000	0.000	0.003	0.764
X_{Mg}	0.609	0.595	0.604	0.687	0.177	0.180	0.447	0.397	0.477	0.462	0.230	0.132	0.224	0.527

*Analyzed by a scanning electron microscope (*CamScan-Cambridge*) equipped with a link energy-dispersive system. The apparatus for energy dispersive analysis does not allow estimation of water and fluorine contents in water-bearing minerals and uses normalization to 100% for all minerals

**Crystallographic formulae are calculated using the cation method: *Pl* per 5 cations, *Grt* per 8 cations, *Bt* per 7 cations, *Chl* per 10 cations, *Hbl* per 13 cations, *Ms* per 6 cations

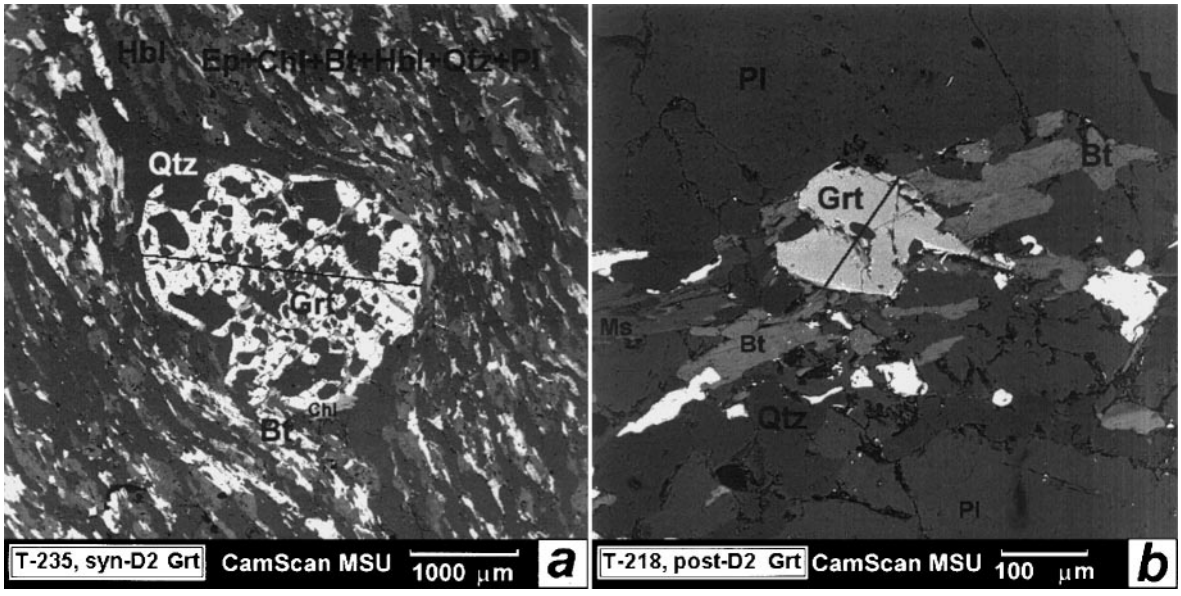

Fig. 7. Morphology of syn-D2 (T-235) (**a**) and post-D2 (T-218) (**b**) garnet porphyroblasts from the metamorphic rocks of the Yukseevskiy complex. Lines show profiles along which detailed microprobe analyses were done (see Fig. 8a, d). Back-scattered electron images were taken with the CamScan electron microscope at the Department of Petrology, Moscow State University

a flat profile with low Mn contents in the core and a decrease in N_{Mg} towards the rim (Fig. 8b, d). This type of garnet is commonly found in gneisses, metabasites and some quartzites, reflecting peak metamorphism as well as the subsequent retrograde history of the rocks. Morphologically and chemically the two types of garnet are very similar to garnets studied in sheared low-grade cratonic rocks bordering the Limpopo Granulite Complex of Southern Africa and the Lapland Granulite Belt of the Kola Peninsula (*Perchuk* et al., 1999).

Two generations of mica could also be distinguished occurring mainly in gneisses and schists of the Yukseyevskiy Complex. A syn-D2 generation defines the main schistosity as well as the shear fabric in the D2 shear zones (Fig. 7a), while a post-D2 generation, represented by randomly oriented flakes of Bt and Ms, are commonly associated with the second generation of garnet (Fig. 7b). An insignificant change in the Ti and Si content from syn- to post-D2 *Bt* could be distinguished (Table 2). All muscovite grains are slightly zoned and demonstrate a decrease in the Na content from core to rim, while biotite in contact with garnet shows an increase in N_{Mg} due to Fe-Mg exchange during a post-peak decrease in temperature. Chlorite in all rock types mainly forms part of post-D2 assemblages (Table 1) and commonly replaces both syn-D2 and post-D2 garnet (Fig. 7a).

Syn-D2 and post-D2 generations of amphibole in metabasic rocks and gneisses were also observed. The syn-D2 generation commonly forms elongated grains oriented along the D2 lineation in coarse-grained (10 mm) amphibolites affected by D2 shearing (e.g. T-244, Table 1). The composition of syn-D2 hornblende is fairly constant and characterized by flat chemical profiles (Fig. 8e). The narrow

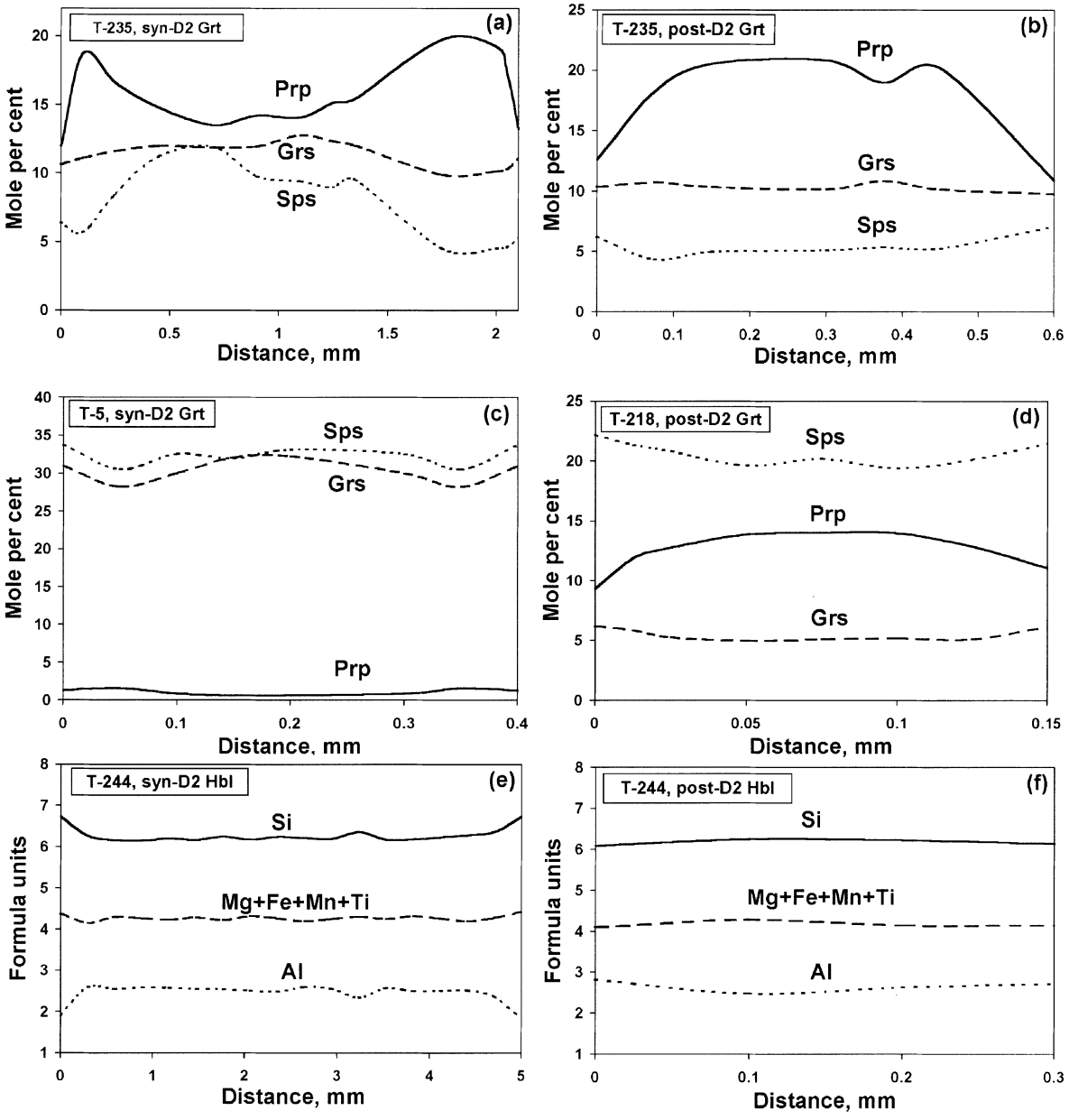

Fig. 8. Comparison of chemical profiles across syn-D2 (**a**, **c**, **e**) and post-D2 (**b**, **d**, **f**) garnets (**a**, **b**, **c**, **d**) and amphiboles (**e**, **f**) from rocks of the Yukseevskiy complex: Formulas of hornblende are calculated per 13 cations

(< 100 Mm) rims of these amphiboles occasionally show a decrease in A1 and an increase in the Si content at the contact with *Pl* and *Qtz* (Table 2, Fig. 8e). No clear reversible zoning was, however, found. This suggests that, in contrast to the syn-D2 garnet that preserved compositional evidences of the prograde stage, most amphiboles were significantly homogenized at peak metamorphic conditions, therefore only reflecting the peak and post-peak events. The post-D2 generation of

hornblende is represented by randomly oriented, small 0.1–0.5 mm grains of amphibole that commonly surround the syn-D2 generation. Their composition is very similar to that of the syn-D2 generation (Table 2, Fig. 8f). In the D3-mylonites, late actinolitic amphibole was found reflecting the greenschist facies conditions of the shear deformation.

Plagioclase also forms two generations differing in their relationship with the D2 shear fabric. The syn-D2 generation is represented by 0.5–1 mm porphyroblasts with clear pressure shadows (T-44a, T-244 in Table 1) as well as by elongated ~ 0.1 mm grains oriented parallel to the D2-shear plane (T-244 in Table 1). Post-D2 plagioclase forms isometric grains associated with other post-D2 minerals. The composition of the two generations of *Pl* do not differ systematically and commonly vary within 1–13 *An* numbers in each sample. Very stable *Pl* compositions ($N_{An} = 0.30$–0.31) were analyzed in garnet-bearing mica schist T-218 (Table 1).

Thus, two major tectonic generations of rock-forming minerals can be distinguished, namely syn-D2 and post-D2 (Table 1). Mg-poor, inclusion-rich cores of some syn-D2 garnets probably represent an earliest pre-D2 (syn-D1) generation (e.g. samples T-235 and T-44a in Table 1). The D3 stage is mainly represented in D3-mylonite zones by the retrogressive development of late chlorite and actinolite in epidote-amphibolite facies parageneses.

P-T conditions of metamorphism and deformation

In order to estimate *P-T* conditions of metamorphism and deformations of the rocks of the Yukseevskiy complex an internally consistent system of geothermometers (*Perchuk*, 1989, 1990) and geobarometers (*Perchuk* et al., 1996; *Gerya* et al., 1997; *Perchuk* and *Krotov*, 1998; *Perchuk* et al., 1999) was used. The same system was used for geothermobarometry of sheared rocks adjacent to granulites of the Limpopo and the Lapland high-grade terrains (see *Perchuk* et al., 1999) allowing the direct comparison of the results of the *P-T* calculations for the three studied areas.

Table 3 contains the results of the pressure and temperature estimates for the studied samples. Temperatures were calculated by using the *Grt-Bt*, *Grt-Chl*, *Grt-Hbl* (*Perchuk*, 1989, 1990), and *Hbl* (*Gerya* et al., 1997) geothermometers. Pressures were estimated using *Grt-Bt-Ms-Qtz* (*Perchuk* et al., 1999), *Hbl* (*Gerya* et al., 1997) and (for independent pressure control) *Grt-Bt-Ms-Qtz-Pl* (*Hoisch*, 1990) geobarometers. The results of the *P-T* calculations consistently suggest peak metamorphic conditions for the rocks of the Yukseevskiy Complex corresponding to $T = 640$–$680\,^{\circ}\mathrm{C}$ and $P = 5.5$–6.1 kbar. As seen from Table 3 syn-D2 minerals were mainly formed during prograde and peak metamorphism while post-D2 minerals crystallized during peak and retrograde metamorphism. It can therefore be concluded that the major stage of D2 shearing in the rocks of the Yukseevskiy complex was associated with prograde and peak metamorphism.

In order to derive *P-T* paths for the rocks of the Yukseevskiy complex samples T-218 and T-244 (Table 1) were used for detailed *P* and *T* calculations. The calculated *PT*-parameters of local mineral equilibria (i.e. individual *P-T* points) were used to construct a *PT*-path for each sample. Derivation of the *PT*-path was

Table 3. *P-T conditions of metamorphism in the Yukseevskiy complex*

Sample	Location	Analyses*				*T*, °C**				*P*, kbar***		
		Bt	*Grt*	*Chl*	*Hbl*	T_1	T_2	T_3	T_4	P_1	P_2	P_3
Syn-D2 minerals (*prograde metamorphism*)												
T-235	Core	–	–	–	5–6	–	–	–	642	–	5.65	–
T-235	Rim	–	–	–	5–5	–	–	–	659	–	5.97	–
T-235	Core	–	–	–	5–12	–	–	–	655	–	5.89	–
T-235	Rim	–	–	–	5–13	–	–	–	648	–	5.79	–
T-235	Cores	3.18	6.11	–	–	657	–	–	–	–	–	–
T-235	Rims	4.12	4.16	–	–	675	–	–	–	–	–	–
T-244	Core	–	–	–	2–7	–	–	–	644	–	5.48	–
T-244	Rim	–	–	–	2–32	–	–	–	661	–	6.02	
Post-D2 minerals (*peak metamorphism*)												
T-218	Cores	6.31	6.28	–	–	621	–	–	–	5.06	–	4.63–5.52
T-218	Cores	4.38	4.44	–	–	643	–	–	–	5.74	–	5.17–6.34
T-255	Cores	54	44	–	–	678	–	–	–	–	–	–
T-255	Cores	2–31	2–25	–	–	634	–	–	–	–	–	–
T-244	Core	–	–	–	5–37	–	–		642	–	5.70	–
T-244	Rim	–	–	–	5–34	–	–		661	–	6.11	–
T-42b	Cores	42	48	–	–	605	–	–	–	–	–	–
T-42b	Cores	–	–	–	2–62	–	–		644	–	5.21	–
T-42b	Rims	–	–	–	2–65	–	–		655	–	5.72	–
T-42b	Cores	–	2–51	–	15	–	–	643	–	–		–
T-235	Core	–	–	–	5–4	–	–	–	651	–	5.62	–
T-235	Rim	–	–	–	5–1	–	–	–	647	–	5.28	–
T-235	Core	–	–	–	5–14	–	–	–	662	–	5.77	–
T-235	Rim	–	–	–	5–15	–	–	–	660	–	6.10	–
T-233	Cores	–	5–65	–	5–69	–	–	642	–	–	–	–
T-233	Cores	–	5.50	–	5–59	–	–	614	–	–	–	–
T-233	Rims	–	5–66	–	5–70	–	–	683	–	–	–	–
Rims of Post-D2 minerals (*retrograde metamorphism*)												
T-218	Rims	6.35	6.37	–	–	546	–	–	–	3.82	–	3.65–5.14
T-218	Rims	4.39	4.40	–	–	589	–	–	–	4.61	–	3.61–4.98
T-255	Rims	52	49	–	–	600	–	–	–	–	–	–
T-255	Rims	2–29	2–28	–	–	587	–	–	–	–	–	–
T-244	Rim	–	–	–	2–40	–	–	–	587	–	4.11	–
T-244	Rim	–	–	–	2–28	–	–	–	610	–	4.76	–
T-244	Rim	–	–	–	5–42	–	–	–	584	–	4.10	–
T-244	Rim	–	–	–	5–43	–	–	–	637	–	5.35	–
T-42b	Rims	–	6	7	–	–	530	–	–	–	–	–
T-42b	Rims	–	56	51	–	–	514	–	–	–	–	–
T-42b	Rims	–	2–53	–	10	–	–	612	–	–	–	–
T-42b	Rims	25	24	–	–	536	–	–	–	–	–	–
T-42b	Rims	38	43	–	–	584	–	–	–	–	–	–

(continued)

Table 3 (*continued*)

T-235	Rims	4.13	4.14	–	–	559	–	–	–	–	–	–
T-235	Rims	4.19	4.20	–	–	602	–	–	–	–	–	–
T-235	Rims	–	3.13	3.15	–	–	557	–	–	–	–	–
T-233	Rims	–	5–51	5–54	–	–	600	–	–	–	–	–
T-233	Rims	–	5–52	5–53	–	–	627	–	–	–	–	–
T-233	Rims	–	5–77	5–78	–	–	622	–	–	–	–	–

*Representative analyses are given in Table 2, other analyses available on request. **Temperatures were calculated using *Grt-Bt* (T_1), *Grt-Chl* (T_2), *Grt-Hbl* (T_3) (*Perchuk*, 1989, 1990) and *Hpl* (T_4) (*Gerya* et al., 1997) geothermometers: T_1 calculated at P_1 where P_1 is given and at $P = 5$ kbar in other cases; T_2 and T_3 calculated at $P = 5$ kbar; T_4 calculated at P_2. ***Pressures were calculated using *Grt-Bt-Ms-Qtz* (*Perchuk* et al., 1999) (P_1), *Hbl* (*Gerya* et al., 1997) (P_2), and *Grt-Bt-Ms-Qtz-Pl* (*Hoisch*, 1990) (P_3) geobarometers: P_1 calculated at T_1; P_2 calculated at P_3 represents minimal and maximal pressures calculated at T_1 using six geobarometers by *Hoisch* (1990). *Hpl* I calculation of P_1 and P_3 analyzed *Pl* and *Ms* compositions were used (see analyses 4.48 and 4.59 for T-218 Table 2)

controlled using isopleths of mineral compositions calculated for studied mineral assemblages: the relationship of the *P-T* path with the isopleths should be consistent with the chemical compositions and zoning of the different textural generations of minerals.

For the garnet-bearing mica schist T-218 the *Grt-Bt* geothermometer (*Perchuk*, 1990) and the semi-empirical *Grt-Bt-Ms-Qtz* geobarometer (*Perchuk* et al., 1999) were applied. Garnet in this sample is post-D2 with a clear decrease in the Mg number from core to rim (Fig. 8d). The results of the *P-T* calculations and a *P-T* path for this sample are given in Fig. 9a. The *P-T* path reflects a decrease in pressure and temperature from peak metamorphism (640 °C, 5.7 kbar) to 550 °C and 3.8 kbar during late- and post-D2 events.

For the porphyroblastic amphibolite T-244 an empirical *Hbl* geothermobarometer (*Gerya* et al., 1997) was applied. Hornblende in this sample is represented by both syn-D2 and post-D2 generations. The results of *P-T* calculations and a *P-T* path for this sample are given in Fig. 9b. The *P-T* path reflects early peak metamorphic conditions (640 °C, 5.6 kbar) recorded by cores of large (up to 10 mm) syn-D2 porphyroblasts. Peak metamorphism (660 °C, 5.9 kbar) corresponds to the formation of relatively actinolite-poor hornblende that constitutes most of the rims of syn-D2 porphyroblasts and euhedral post-D2 < 300 μm grains. The retrograde part of the path to $T = 580$ °C and $P = 4.1$ kbar is recorded by relatively actinolite-rich zones at the contact of both syn-D2 and post-D2 *Hbl* with plagioclase and quartz (Fig. 8e). The pressure and temperature estimates for mica schists and amphibolites coincide well (Table 3, Fig. 9a, b), suggesting consistency of the thermobarometers used. Pressure estimates obtained using the *Grt-Bt-Ms-Qtz* geobarometer (*Perchuk* et al., 1999) for sample T-218 are also consistent with those calculated using the geobarometers of *Hoisch* (1990) (Table 3). In *P-T* space both *P-T* paths are located in the sillimanite stability field. This is consistent with the presence of *Sil* in some of the garnet-free mica schists of the Yukseevskiy Complex (*Gerya* et al., 1986) while *Ky* has never been described from these rocks.

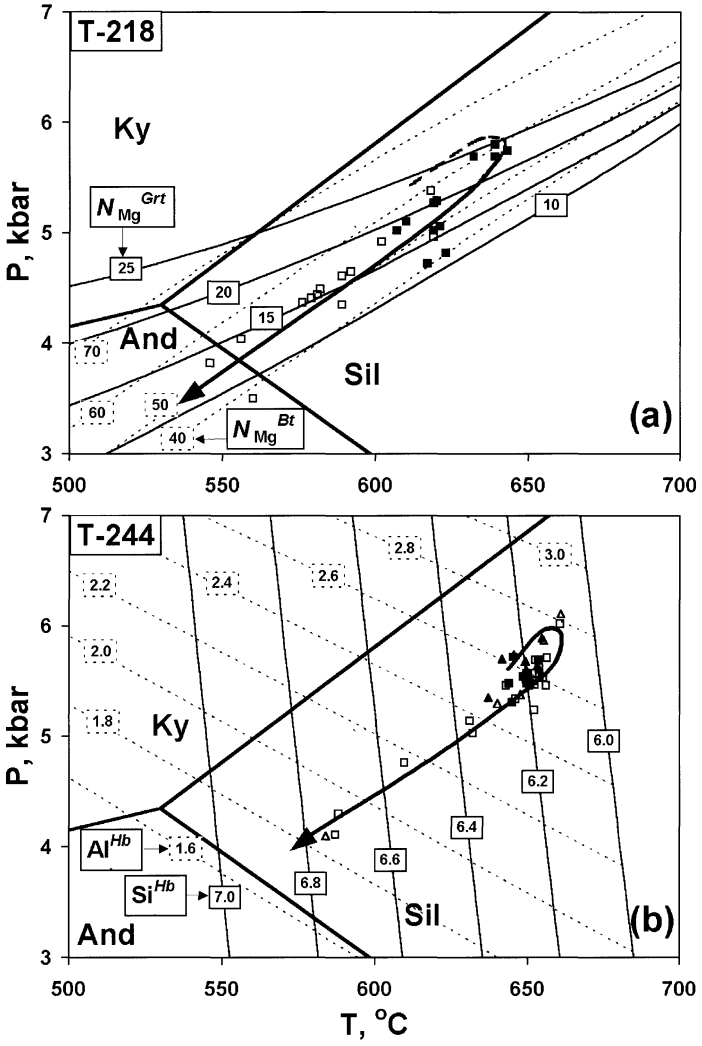

Fig. 9. *PT*-paths derived for the samples of mica schist (**a**) and metabasite (**b**) of the Yukseevskiy complex. Symbols denote individual *P-T* estimations: open symbols show *P-T* parameters calculated using compositions of cores while solid symbols denote those for rims. **a** mica schists T-218 (Table 1); individual *P-T* parameters and N_{Mg} isopleths of *Grt* and *Bt* calculated using *Grt-Bt* geothermometer (*Perchuk*, 1989, 1990), *Grt-Bt-Ms-Qtz* geobarometer (*Perchuk*, 1999) and compositions of coexisting post-D2 *Grt*, *Bt* and *Ms* (see Table 2, 3). **b** amphibolite T-244 (Table 1); individual *P-T* parameters and isopleths of Si and Al in *Hbl* (per 13 cations, at $N_{Mg}^{Hbl} = 60$) calculated using the *Hbl* geothermobarometer (*Gerya* et al., 1997) and compositions of syn-D2 (rectangles) and post-D2 (triangles) amphiboles (see Tables 2, 3)

Detailed investigations of metapelites of the Kanskiy Complex (*Perchuk* et al., 1989) revealed decompression (first stage) followed by near isobaric cooling of the granulites. Individual samples yielded *P-T* paths ranging from 100 °C/kbar to 140 °C/kbar (Fig. 10) depending on their location with respect to the Tarakskiy pluton. The steeper slopes of *P-T* paths (100 °C/kbar) are characteristic of the

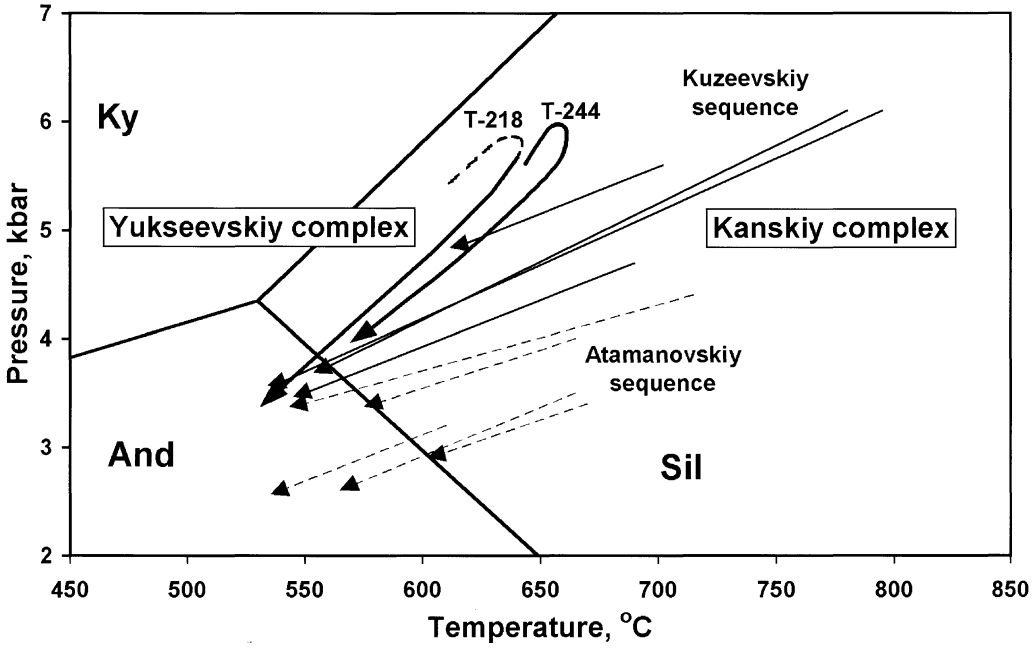

Fig. 10. Joint *P-T* evolution of granulites of the Kuzeevskiy (solid thin arrows) and Atamanovskiy (dashed thin arrows) sequences of the Kanskiy Complex (*Perchuk* et al., 1989) and of adjacent greenstone belt rocks (solid thick arrows) of the Yukseevskiy complex (this study)

samples taken close to the Tarakskiy pluton. This is explained by the faster uplift of the rocks that were involved in the granite-gneiss dome structure. Calculated *P-T* paths differ in pressure (Fig. 10) suggesting that near-isobaric cooling occurred at different depths in different parts of the Kanskiy complex. Maximum depths (15–18 km) of near-isobaric cooling are characteristic for the rocks of the Kuzeevskaya sequence in the western margin of the Kanskiy complex (localities B and C in Fig. 1b). Minimum depths (8–11 km) of the cooling were calculated for metapelites of the Atamanovskaya sequence from the NE part of the complex (locality A in Fig. 1b).

The retrograde *P-T* paths (Fig. 10) of the rocks of the Yukseevskiy Complex coincide with the minimum *T* of the near-isobaric cooling *P-T* paths for the adjacent granulites of the Kuzeevskiy sequence of the Kanskiy Complex (*Perchuk* et al., 1989). This suggests the presence of a high temperature gradient between the exhuming granulites and the adjacent greenstone belt rocks of the Yukseevskiy and Yeniseyskiy Complexes. Therefore, the exhuming granulites presumably provided a heat source for the metamorphism of the adjacent greenstone belt rocks during their emplacement. As a result, greenstone rocks were progressively metamorphosed during the D2 stage. Peak metamorphism and exhumation of these rocks correspond to the late- and post-D2 history.

The studied relationship between the *P-T* paths of the granulites and the adjacent greenstone belt rocks of the Southern Yenisey Range are similar to those (*Perchuk* et al., 1999) observed in metamorphic complexes of South Africa

(Limpopo area) and the Kola Peninsula (Lapland area). This suggests similar geodynamic histories for all three terrains.

Discussion

Zones bordering granulite complexes are common sites of juxtaposed low-grade (e.g. greenstone belts) and high-grade terrains. Such sites can be studied in terms of their temporally related rock types, tectonic setting and metamorphic history in order to develop a geodynamic model for the formation of such juxaposed terrains. The Southern Yenisey Range has the following characteristics in this regard:

Lithologies

The major rock types of the high-grade Kanskiy Complex are geochemically and petrochemically very similar to those of Archaean greenstone belts (*Nozkhin* and *Turkina*, 1993). The Yukseevskiy Complex also demonstrates rock associations, metamorphic, petrological and geochemical features typical of Archaean greenstone belts. This would suggest that lithologies from the low- and high-grade terrains of the Yenisey Range could be genetically related, as has been shown in the case of the Limpopo Belt (*Kreissig* et al., 2000).

Structure

The regional low-grade D1 schistosity observed throughout the greenstone terrain represents an early event that predates the emplacement of the Kanskiy Complex. The onset of a NNW directed D2 thrust event observed along the western margin of the Yukseevskiy Complex progressed eastwards into larger D2 shear zones that finally culminates in a regional shear zone up to 1 km wide on the boundary between the Yeniseyskiy and Kanskiy Complexes (Fig. 1b). D2 kinematic indicators in these shear zones suggest a consistent top to the NNW thrust movement across the entire study area. This progressive increase in shear deformation suggests that compressional forces were operative in a roughly east-west direction during the emplacement of the Kanskiy granulite Complex. Kinematic indicators in D2 shear zones in the western part of the Southern Yenisey Range suggest a consistent top to the NNW thrust movement. This uniform structural pattern across the Southern Yenisey Range however, changes dramatically as the contact with the high-grade Kanskiy Complex is reached suggesting top to the SW movement. Exactly how this systematic change in the stress field towards the Kanskiy Complex developed is not entirely clear. The rheological characteristics of hanging and footwall sections of such large-scale shear zones would differ significantly and could contribute towards a deviation in the transport direction. This is supported by the differences in tectonic pattern detected within this zone for the granulites of the Kanskiy complex (weak foliation and lineation and intensive folding) and in the gneisses and amphibolites of the Yeniseyskiy complex (strong foliation and lineation and weak folding), probably suggesting relative plasticity of the overthrusted granulites and relative stiffness of the underthrusted gneisses and amphibolites. Late D3-shear event corresponds to

development of a system of mylonite shear zones characterized by near *horizontal* mineral stretching lineations with dextral strike-slip movement.

Metamorphism

The systematic increase in the grade of metamorphism in the Yukseevskiy and Yeniseyskiy Complexes towards the border of the Kanskiy Complex can be related to the so called ≪hot iron effect≫ of the overthrusted hot rocks very similar to that described from the underthrusted granite-greenstone rocks along the southern boundary of the Limpopo Granulite Belt of Southern Africa (*Van Reenen* and *Smit*, 1996). The granulites of the Kanskiy Complex therefore provided the heat source for prograde metamorphism in the Yeniseyskiy and Yukseevskiy Complexes as is reflected by a regional dynamic metamorphic zonation. The rocks of the Yukseevskiy complex experienced prograde, peak ($\sim 660\,^{\circ}C$ and ~ 5.8 kbar) and partially retrograde metamorphism during the D2 events. The intense cooling of the granulites during their emplacement is supported by widely developed near isobaric cooling reaction textures and *P-T* paths developed in metapelites of the Kanskiy Complex (*Perchuk* et al., 1989). A similar scenario is also suggested for the well studied Limpopo Belt (*Van Reenen* and *Hollister*, 1988; *Baker* et al., 1992; *Van Schalkwyk* and *Van Reenen*, 1992).

Tectonic interpretation

The geological relationship of metamorphic complexes of the Southern Yenisey Range is virtually identical to that described for the Limpopo Granulite Complex (Southern Africa) and the Lapland granulite Complex (Kola Peninsula), therefore favoring a geodynamic model that differs from the published accreted terrain model of the area (e.g. *Kovrigina*, 1973, 1977; *Dacenko*, 1995). The results of our study suggest that at 2000–1800 Ma (*Bibikova* et al., 1993) continued thrusting during the extrusion of the hot granulites of the Kanskiy Complex onto the colder greenstone rocks of the adjacent Yeniseyskiy and Yukseevskiy Complexes along outward verging ductile thrusts in the marginal footwall resulted in a coherent syn-shearing structural and metamorphic framework for the Southern Yenisey Range. The dynamic forces that caused the deformation of the Southern Yenisey Range could be attributed to a collisional type model as has, for instance, been suggested to explain the relationship between the high-grade Limpopo Belt and the granite-greenstone terrain of the adjacent Kaapvaal Craton (*De Wit* et al., 1992; *Roering* et al., 1992a, b; *Smit* and *Van Reenen*, 1997). It could, however, also be explained by the gravitational redistribution model (*Perchuk*, 1989; *Perchuk* et al., 1992, 1997; *Perchuk* and *Gerya*, 1995) as recently applied to the evolution of both the Limpopo and Lapland granulite terrains and their associated granite greenstone belts (*Perchuk* et al., 1999).

The D3 mylonitization event, on the other hand, is probably related to large-scale mylonitic shear zones (Fig. 1a, b) that occur across the entire Yenisey Range, dated at 1450 Ma by *Nozkhin* et al. (1989).

Based on this data a preliminary tectono-metamorphic scheme of crustal evolution of the complexes of the Southern Yenisey Range is proposed (Table 4).

Table 4. *Tectono-metamorphic framework for the evolution of the Southern Yenisey Range*

Stage	Age	Kanskiy	Yeniseyskiy	Yukseevskiy
D1	> 1900 Ma[1, 2]	Regional D1 foliation, prograde granulite facies metamorphism	Regional D1 foliation, prograde epidote amphibolite to amphibolite facies metamorphism	Regional D1 foliation, prograde greenschists to epidote amphibolite facies metamorphism
D2	~ 1900 Ma[1, 2, 3]	D2-shearing, exhumation (thrusting) of the complex, retrograde granulite to amphibolite facies metamorphism, near isobaric cooling of granulites, Tarakskiy granite emplacement.	D2-shearing, peak deformation, peak and retrograde amphibolite to epidote-amphibolite facies metamorphism.	D2-shearing prograde peak, and retrograde epidote- amphibolite facies metamorphism
D3	< 1900 Ma[1, 2] (probably 1450 Ma[2])	D3 mylonitization greenschist to epidote-amphibolite facies metamorphism	D3 mylonitization greenchist to epidote-amphibolite facies metamorphism	D3 mylonitization greenchist facies metamorphism

[1]*Bibikova* et al. (1993); [2]*Nozkhin* et al. (1989); [3]*Gerling* and *Artemov* (1964); *Volobuev* et al. (1976)

Conclusions

Combined structural and petrological studies of the epidote-amphibolite to amphibolite facies metamorphic Yukseevskiy and Yeniseyskiy complexes adjacent to the granulites of the Kanskiy complex in the Southern Yenisey Range provided important new data on their tectono-metamorphic relationships. All the complexes are characterized by a uniform D2-shear pattern that formed due to the exhumation of the Kanskiy complex at 2000–1800 Ma. The granulites were thrusted along a regional ductile shear zone onto the lower grade rocks causing deformation accompanied by prograde metamorphism. The retrograde *P-T* path of the Yukseevskiy Complex coincides with the minimum *T* of the near-isobaric cooling *P-T* paths for the adjacent granulites of the Kanskiy Complex (*Perchuk* et al., 1989).

These relationships are similar to those (*Perchuk* et al., 1999) observed in metamorphic complexes of South Africa (Limpopo area) and the Kola Peninsula (Lapland area), suggesting that the exhumation of high-grade terrains in the Early Precambrian could be related to similar geodynamic processes.

Acknowledgments

Since 1995 this work was carried out as part of the Russia-South Africa collaboration supported by FRD (Foundation for Research Development) Gencor and JCI grants to *DDvR*. We are grateful *L. L. Perchuk* (Moskow State University) for discussing the results and for his valuable suggestions. The manuscript was much improved due to critical reviews by *K. Stüwe* and *I. Scrimgeour.*

References

Baker J, Van Reenen DD, Van Schalkwyk JF, Newton RC (1992) Constraints on the composition of fluids involved in retrograde anthophyllite formation in the Limpopo Belt, South Africa. Precamb Res 55: 327–336

Bibikova EV, Gracheva TV, Makarov VA, Nozkhin AD (1993) Age boundaries in the geological evolution of Early Precambrian of Yenisey Range. News of Russian Academy of Sciences, Stratigraphy and geological correlations 1: 35–40 (in Russian)

Dacenko VM (1984) Granitoid magmatism of south-western environment of Siberian platform. SNIIGGIMS press, Novosibirsk, 120 pp

Dacenko VM (1995) Niznekanskiy massif – a standard of Niznekanskiy granitoid Complex (Yenisey Range). SNIIGGIMS press, Novosibirsk, 123 p (in Russian)

De Wit MJ, Roering C, Hart RJ, Armstrong RA, De Ronde CEJ, Green RWE, Tredoux M, Pederdy E, Hart RA (1992) Formation of an Archaean continent. Nature 357: 553–562

Gerling EK, Artemov YuM (1964) Absolute geochronology of south and central parts of the Yenisey range. Geochemistry 7: 610–622 (in Russian)

Gerya TV, Dacenko VM, Zablotskiy KA, Kornev TYa, Lepezin GG, Nozkhin AD, Popov NV, Reverdatto VV, Shvedenkov GYu (1986) Precambrian crystalline complexes of the Yenisey Range. Institute of Geology and Geophysics Siberian Branch USSR Academy of Sciences, Novosibirsk, 120 p (in Russian)

Gerya TV, Perchuk LL, Triboulet C, Audren C, Sez'ko AI (1997) Petrology of the Tumanshet metamorphic complex, eastern Sayan, Siberia. Petrology 5(6): 503–533

Hoisch D (1990) Empirical calibration of six geobarometers for the mineral assemblage quartz + muscovite + biotite + plagioclase + garnet. Contrib Mineral Petrol 104: 225–234

Kovrigina EK (1973) Petrology of metamorphic sequences of Early Precambrian Angaro-Kanskiy part of the Yenisey Range. Thesis, VSEGEI Press, Leningrad, 27 p (in Russian)

Kovrigina EK (1977) Tectonics of the Angaro-Kanskiy part of the Yenisey Range. Reports on tectonics and magmatism of Siberia. VSEGEI Press, Leningrad, pp 24 – 40 (in Russian)

Kreissig K, Nogel TF, Kramers JD, Van Reenen DD, Smit CA (2000) An isotopic and geochemical study of the northern Kaapvaal Craton and the Southern Marginal Zone of the Limpopo Belt: are they juxtaposed terranes? Lithos (in press)

Kusnetsov YuA (1941) Petrology of the Yenisey Range. Data on geology of Western Siberia, Tomsk, 15(57) (in Russian)

Kusnetsov YuA (1988) Selected works. V. I. Petrology of the Precambrian of the Southern Yenisey range. Nauka Press, Novosibirsk, 220 p (in Russian)

Mints MV, Glaznev VN, Konilov AN, Kunina NM, Nikitichev AP, Raevsky AB, Sedikh YuN, Stupak VM, Fonarev VI (1996) The Early Precambrian of the North-Eastern Baltic shield: paleodynamics, crustal structure, and evolution. Sci World, Press Moscow, 312 p (in Russian)

Nozkhin AD (1983) Early Precambrian gneiss complexes of the Yenisey Range and their geochemical peculiarities. Geol Geophys 9: 3–11 (in Russian)

Nozkhin AD (1985) Early Precambrian trough complexes of the South-Western part of the Siberian platform and its metallogeny. In: Precambrian trough structures of the Baykal-Amur region and its metallogeny. Nauka Press, Novosibirsk, pp 34 – 46 (in Russian)

Nozkhin AD (1997) Petrogeochemical typization of Precambrian complexes of the South of Siberia. Thesis, Institute of Geology, Geophysics and Mineralogy Siberian Branch Russian Academy of Sciences, Novosibirsk, 99 p (in Russian)

Nozkhin AD, Turkina OM (1993) Geochemistry of granulites. Reports of Institute of Geology and Geophysics Russian Academy of Sciences, Novosibirsk 817: 224 pp (in Russian)

Nozkhin AD, Malishev VI, Sumin AV, Ostapenko EI, Gerya TV (1989) Age of metamorphic complexes in south-western part of Siberian platform after the data of Pb-isotopic studies. Geol Geophys 1: 13–22 (in Russian)

Passchier CW, Trouw RA (1996) Microtectonics. Springer, Berlin Heidelberg New York Tokyo, 289 p

Perchuk LL (1989) P-T-fluid regimes of metamorphism and related magmatism with specific reference to the Baikal Lake granulites. In: *Daly JS, Yardley BWD, Cliff BO* (eds) Evolution of metamorphic belts. Geol Soc London, Spec Publ 42(20): 275–291

Perchuk LL (1990) Derivation of thermodynamically consistent system of geothermometers and geobarometers for metamorphic rocks and magmatic. In: *Perchuk LL* (ed) Progress in metamorphic and magmatic petrology. Cambridge Univ Press, Cambridge, pp 93–112

Perchuk LL, Gerya TV (1995) Studies of the boundaries between granulite facies terrains and cratons. Contennial Geocongress. Extended Abstracts. The Geol Soc South Africa 2: 622–623

Perchuk LL, Krotov AV (1998) Petrology of the mica schists of the Tanaelv belt in the southern tectonic framing of the Lapland granulite complex. Petrology 6: 149–179

Perchuk LL, Gerya TV, Nozhkin AD (1989) Petrology and retrogression in granulites of the Kanskiy Formation, Yenisey Range, Eastern Siberia. J Metamorph Geol 7: 599–617

Perchuk LL, Podladchikov YuYu, Polaykov AN (1992) Geodynamic modeling of some metamorphic processes. J Metamorph Geol 10: 311–318

Perchuk LL, Gerya TV, Van Reenen DD, Safonov OG, Smit CA (1996) The Limpopo metamorphic complex, South Africa. 2. Decompression/cooling regimes of granulites and adjusted rocks of the Kaapvaal craton. Petrology 4: 571–599

Perchuk LL, Gerya TV, Van Reenen DD, Smit CA (1997) Cratonization: from greenstone belts to granulites. Terra abstracts (EUG 9). Terra Nova [Suppl 1] 9: 362 (Abstract)

Perchuk LL, Gerya TV, Van Reenen DD, Smit CA, Krotov AV (1999) *P-T* paths and tectonic evolution of shear zones separating high-grade terrains from cratons: examples from Kola Peninsula (Russia) and Limpopo region (South Africa). Mineral Petrol (this volume)

Pozhilenko VI, Smolkin VF, Sharov NV (1997) Seismic-geological models for the Earth's crust in the Lapland-Pechenga region, Russia. In: *Sharov NV* (ed) A seismological model of the Lithosphere of northern Europe: Lapland-Pechenga. Region). Russian Academy of Sciences, Kola Scientific Center Apatity, pp 181–208 (in Russian)

Roering C, Van Reenen DD, de Wit MJ, Smit CA, de Beer JH, Van Schalkwyk JF (1992a) Structural geological and metamorphic significance of the Kaapvaal Craton – Limpopo Belt contact. Precamb Res 55: 69–80

Roering C, Van Reenen DD, Smit CA, Barton JM Jr, de Beer JH, De Wit MJ, Stettler EH, Van Schalkwyk JF, Stevens G, Pretorius S (1992b) Tectonic model for the evolution of the Limpopo Belt. Precamb Res 55: 539–552

Serenko VP (1969) New data on metamorphism of the southern part of the Yenisey Range. Geol Geophys 9: 136–141 (in Russian)

Simpson C (1986) Determination of movement sense in mylonites. J Geol Education 34: 246–261

Simpson C, Schmid SM (1983) An evaluation of criteria to deduce the sense of movement in sheared rocks. Geol Soc Am Bull 94: 1281–1288

Smit CA, Van Reenen DD (1997) Deep crustal shear zones, high-grade tectonites and associated alteration in the Limpopo belt, South Africa: implication for deep crustal processes. J Geol 105: 37–57

Van Reenen DD, Hollister L (1988) Fluid-inclusions in hydrated granulite facies rocks. Southern Marginal Zone of the Limpopo belt, South Africa. Geochim Cosmochim Acta 52: 1057–1064

Van Reenen DD, Smit CA (1996) The Limpopo Metamorphic Belt, South Africa. 1. Geological setting and relationship of the Granulite Complex with the Kaapvaal and Zimbabwe Cratons. Petrology 4/6: 562–570

Van Reenen DD, Roering C, Brandl G, Smit CA, Barton JM Jr (1990) The granulite facies rocks of the Limpopo belt, southern Africa. In: *Vielzeuf D, Vidal Ph* (eds) Granulites and crustal evolution. Kluwer, Dordrecht, pp 257–289 (NATO Asi series)

Van Schalkwyk JF, Van Reenen DD (1992) High-temperature hydration of the granulites from the Southern Marginal Zone of the Limpopo Belt by infiltration of CO_2-rich fluid. Precamb Res 55: 337–352

Volobuev MI, Zikov SI, Stupnikova NI (1976) Geochronology of Precambrian formations of the Sayan–Yenisey region of Siberia. In: Actual questions of modern geochronology. Nauka Press, Moscow, pp 96–123 (in Russian)

Volobuev MI, Zikov SI, Stupnikova NI, Vorob'ev IV (1980) Pb-isotopic geochronology of Precambrian metamorphic complexes of South-Western boundary of Siberian platform. In: Geochronology of Eastern Siberia and Far East. Nauka Press, Moscow, pp 14–30 (in Russian)

Authors' addresses: Dr. *A. Smit* and Dr. *D. D. Van Reenen*, Department of Geology, Rand Afrikaans University, Auckland Park, 2006 South Africa, e-mail: casm@na.rau.ac.za; ddvr@na.rau.ac.za; Dr. *T. V. Gerya*, Dr. *D. A. Varlamov* and Dr. *A. V. Fed'kin*, Institute of Experimental Mineralogy, Russian Academy of Sciences, Chermogolovka, Moscow district, 142432 Russia, e-mail: taras@iem.ac.ru